Spring 2016

Behavioral Characterization of a Knock-in Mouse Model of Huntington's Disease

Shawn Minnig
Western Washington University, shawnminnig@gmail.com

Behavioral Characterization of a Knock-in

Mouse Model of Huntington's Disease

By

Shawn Minnig

Accepted in Partial Completion
Of the Requirements for the Degree
Master of Science

Kathleen L. Kitto, Dean of the Graduate School

ADVISORY COMMITTEE

Chair, Dr. Jeffrey Carroll

Dr. Jeffrey Grimm

Dr. Larry Symons

MASTER'S THESIS

In presenting this thesis in partial fulfillment of the requirements for a master's degree at Western Washington University, I grant to Western Washington University the non-exclusive royalty-free right to archive, reproduce, distribute, and display the thesis in any and all forms, including electronic format, via any digital library mechanisms maintained by WWU.

I represent and warrant this is my original work, and does not infringe or violate any rights of others. I warrant that I have obtained written permissions from the owner of any third party copyrighted material included in these files.

I acknowledge that I retain ownership rights to the copyright of this work, including but not limited to the right to use all or part of this work in future works, such as articles or books.

Library users are granted permission for individual, research and non-commercial reproduction of this work for educational purposes only. Any further digital posting of this document requires specific permission from the author.

Any copying or publication of this thesis for commercial purposes, or for financial gain, is not allowed without my written permission.

Shawn Minnig
May 2016

Behavioral Characterization of a Knock-in Mouse Model of Huntington's Disease

A Thesis
Presented to
The Faculty of
Western Washington University

In Partial Fulfillment
Of the Requirements for the Degree
Master of Science

By
Shawn Minnig
May 2016

Abstract

Huntington's disease (HD) is a progressive, fatal neurodegenerative disease caused by an inherited CAG expansion on the Huntingtin (*HTT)* gene resulting in cognitive, affective, and motor related symptoms. Although clinical diagnosis depends on the presence of Huntington's chorea, a movement disorder consisting of irregular movements, cognitive symptoms appear 10-15 years prior during the pre-manifest stage of the disease and are more debilitating to patients. One of the most important advances in HD research has been the generation of mouse models that recapitulate the features of human HD, allowing researchers to identify the pathogenic mechanisms associated with the disease and test the potential therapeutic treatments. Unfortunately, many treatments that have been successful in mouse models have failed to translate to humans when tested in pre-clinical trials. This is partly because experimenters have largely focused on improving late-stage features of HD such as cell death and motor dysfunction, and utilized transgenic mouse that are severely impaired but poorly reproduce the pathogenic processes that underlie the disease. In contrast, knock-in (KI) mouse models are genetically faithful to the human condition but remain underutilized in pre-clinical research due to their slower progression and subtle overt phenotype. This thesis characterized the behavioral deficits associated with the $Htt^{Q111/+}$ KI mouse model of HD and discovered novel cognitive phenotypes that are characteristic of the pre-manifest stage of the disease. At nine months of age, $Htt^{Q111/+}$ mice display improved procedural memory on the two-cue MWM, hypoactivity, reduced velocity, and increased anxiety during open field exploration, and intact spatial LTM with a reduction in the total number of investigations toward both objects during an object location task. Together, these tasks provide a number of robust behavioral phenotypes for use in pre-clinical research conducted in the $Htt^{Q111/+}$ mouse model of HD in the future.

Table of Contents

Abstract……...iv

List of Figures and Tables…….……vi

Introduction…….…….....1

Methods…….…….…….…….....….22

Ethical considerations……..…….…….…22

Experimental animals……..……...22

Two-cue Morris water maze……..…….…….…22

Shaping and one-cue training.…..……....…….....23

Two-cue training and probe trials…….…….....…...24

Open field…….……..…….……...…...26

Object location task……...…….....…...27

Statistical analyses……... ……...….28

Results……..…….…….29

Two-cue Morris water maze training trials…….....……...…...29

Two-cue Morris water maze probe trials……...……....…....29

Open field……....……...30

Object location task……....31

Discussion……..……...…….32

References……..……...….43

List of Figures and Tables

Table 1. Mean latencies to locate the escape platform during two-cue MWM training by day.

Figure 1. Schematic of the direct, indirect, hyper-direct, and dopaminergic projections within the basal ganglia.

Figure 2. Schematic of the gradient of pathology observed during early manifest HD.

Figure 3. Schematic of the eight possible MWM orientations and entry locations.

Figure 4. Visual representation of the concentric zones used to measure thigmotaxis in experimental animals.

Figure 5. Average latency to reach the escape platform during two-cue Morris water maze training trials by day.

Figure 6. Percentage of total time spent in the goal and lure quadrants during two-cue MWM probe trials.

Figure 7. Total distance traveled (cm) by $Htt^{+/+}$ and $Htt^{Q111/+}$ mice during the OF session.

Figure 8. Total time spent actively exploring by $Htt^{+/+}$ and $Htt^{Q111/+}$ mice during the open field session.

Figure 9. Average velocity (cm/s) of $Htt^{+/+}$ and $Htt^{Q111/+}$ mice during the open field session.

Figure 10. Percentage of total time spent along the wall by $Htt^{+/+}$ and $Htt^{Q111/+}$ mice during the open field session.

Figure 11. Percentage of total investigations by $Htt^{+/+}$ and $Htt^{Q111/+}$ mice to the familiar and relocated objects during the OLT.

Figure 12. Total number of investigations to the familiar and relocated objects by $Htt^{+/+}$ and $Htt^{Q111/+}$ mice during the OLT

Behavioral Characterization of a Knock-In Mouse Model of Huntington's Disease

Huntington's disease (HD) is a fatal neurological disorder characterized by cognitive decline, affective disturbances, and progressive motor dysfunction (Walker, 2007). The most prominent symptom is chorea, an involuntary movement disorder consisting of brief, irregular movements (Papoutsi, Labuschagne, Tabrizi, & Stout, 2014). HD is caused by a coding cytosine-adenine-guanine (CAG) expansion on the Huntingtin (*HTT)* gene, where repeat lengths above 41 results in full penetrance of the disease (The Huntington's Disease Collaborative Research Group, 1993). A relationship exists between the length of the CAG expansion and the presentation of symptoms such that individuals who express a longer mutation are prone to an earlier onset of the disease (Penney, Vonsattel, MacDonald, Gusella, & Myers, 1997). Prevalence of HD is conservatively estimated at 5-7 cases per 100,000 people (Walker, 2007).

During the late 19th century, George Huntington became the first to describe the nature of the disease that now bears his name (Huntington, 1872). Upon receiving his medical degree from Columbia University, Huntington returned to Long Island, New York to join the family practice where both his father and grandfather had served collectively for 78 years. During that span, the Huntington family treated multiple generations of families afflicted by the lethal movement disorder known now as Huntington's chorea (Dunlap, 1927). Based on his longitudinal observations, Huntington (1872) published his first scientific paper titled "On Chorea" where he documented several central features of the disease including late manifestation, impairment of the mind, a tendency toward suicide, and the involuntary movement disorder that he deemed "hereditary chorea."

Though Huntington was unaware of the pathophysiological mechanisms that cause the disease, he did accurately identify a number of key symptoms that define the illness. Motor

abnormalities are the most recognizable feature, and clinical diagnosis of the disease depends on the presence of motor symptoms that are determined by a clinician to be "unequivocal signs of HD" as measured by the Unified Huntington's Disease Rating Scale (UHDRS), the most commonly used clinical scale in HD (Loy & McCusker, 2013; Reilman, Leavitt, & Ross, 2014). However, the genetic mutation responsible for the disease also leads to affective disturbances including anxiety and depression, progressive psychiatric symptoms, reduced energy metabolism, and cognitive decline (Papoutsi et al., 2014; Walker, 2007). Importantly, cognitive deficits are often described by patients as being more debilitating than motor abnormalities overall, and are highly predictive of both functional decline (Papoutsi, et al., 2014) and future nursing home placement (Paulsen, 2011). Cognitive decline is detectable up to 20 years prior to the onset of motor dysfunction, but most often appears in the 10-year span leading up to clinical diagnosis of the disease (Papoutsi et al., 2014; Paulsen, 2011).

Cognitive deficits in HD generally fall into two categories, those that occur prior to the manifestation of motor symptoms and those that occur after the disease has been clinically diagnosed (Giralt, Saavedra, Alberch, & Perez-Navarro, 2012). Symptoms that arise during the prodromal phase of HD - or prior to the onset of motor dysfunction - generally include impairment in executive function (e.g. working memory, reasoning, planning, and execution), strategy shifting, procedural learning, motor learning (Giralt et al., 2012) and emotional recognition (Labuschagne et al., 2013; Novak et al., 2012). During the manifest stage of HD - or following the onset of motor symptoms - deficits in recognition memory, spatial learning, and difficulties recalling episodic memories begin to emerge (Giralt et al., 2012).

Alterations to the circuitry of cortico-striatal neuronal networks are responsible for the earliest cognitive deficits observed in HD. Recognition that the corpus striatum (i.e. the caudate

nucleus, putamen, and globus pallidus) of HD patients is profoundly affected first gained acceptance during the early 20th century (Vonsattel, 1985). In 1911, Alzheimer noted that neurodegenerative processes are apparent in the cerebral cortex of brains affected by HD, but considered them unlikely to be the anatomic basis of Huntington's chorea since other diseases that cause excessive damage to the cortex fail to elicit the same pattern of deficits (Dunlap, 1927). To uncover the relationship between sub-cortical neurodegeneration and the pattern of deficits observed in HD, Dunlap performed an exhaustive study on the brains of 17 known HD patients and 12 probable cases for which the family history was unclear. Although limited in the scientific tools available to him during his era, Dunlap correctly identified a number of the central neuropathological features of the disease which hold true to this day, such as profound neurodegeneration of the caudate and putamen, atrophied neuropil, reduced brain weight, progressive gliosis, and cerebellar preservation (Dunlap, 1927).

Medium spiny neurons (MSNs) sensitive to gamma-aminobutyric acid (GABA) comprise 90-95% of the neuronal population within the corpus striatum and are the most severely affected cellular subtype in HD. To delineate the progression and features of neurodegeneration within the basal ganglia over time, Vonsattel et al. (1985) evaluated the half-brain specimens of 163 clinically diagnosed HD patients and assigned a disease severity grade to each. At the earliest stages, microscopic evaluations revealed cellular loss of MSNs within the medial portion of the caudate nucleus (with the tail showing more severe neurodegeneration than the head), as well as slight neurodegeneration within the dorsal putamen and moderate fibrillary astrocytosis. Throughout the progression of the disease, cellular loss and astrocytosis becomes more severe in both the striatum and surrounding subcortical structures, ultimately progressing in a dorsal to

ventral, medial to lateral, and caudo-rostral fashion within the basal ganglia (Lawrence, Sahakian, & Robbins, 1998; Papoutsi et al., 2014).

Anatomically, the basal ganglia are composed of five interconnected nuclei: caudate, putamen, globus pallidus (GP) – distinguished by an internal (GPi) and external (GPe) segment, subthalamic nucleus (STN), and the substantia nigra (SN) – subdivided into the pars compacta (SNpc) and pars reticulata (SNpr) (Mink, 1996). The striatum (i.e. the caudate and putamen) is the primary input into the basal ganglia, and receives excitatory glutamatergic afferents from nearly all areas of the cerebral cortex except for primary visual and auditory areas (Mink, 1996). Output from the striatum is composed mainly of inhibitory GABAergic MSNs and is anatomically sub-divided into a "direct" and "indirect" pathway which have opposing effects on thalamic output back to the cerebral cortex (Cohen & Frank, 2009; Mink, 1996). Together, the two pathways act as a selection hub, facilitating desired actions and suppressing unwanted ones via a push/pull type gating mechanism comprised of multiple partially overlapping closed circuit feedback loops (Cohen & Frank, 2009; Mink, 1996). For a schematic of basal ganglia anatomy, see Figure 1.

Direct and indirect pathway MSNs are identifiable by the types of dopamine receptors and neuropeptides they express, as well as the subcortical nuclei they preferentially project to (Chen, Wang, Cepeda & Levine, 2013). Direct pathway MSNs express primarily D_1 receptors, substance P, dynophorin, and project monosynaptically onto the GPi and SNr (Chen et al., 2013; Cohen & Frank, 2009; Deng et al., 2004). Activation of direct pathway MSNs provide focused inhibitory input onto the GPi and SNr, which subsequently disinhibit the thalamus and provide a net excitatory effect upon cortical activity via bottom up thalamocortical drive (Cohen & Frank, 2009). Indirect pathway MSNs, in contrast, express primarily D_2 receptors, enkephalin,

adenosine A_{2A} receptors (Deng et al., 2004), and send polysynaptic inhibitory efferents onto the GPe. The GPe both tonically inhibits the GPi via direct focused projections (Cohen & Frank, 2009), and projects inhibitory axon collaterals onto the STN, which in turn sends excitatory glutamatergic projections onto the GPi and SNr (Chen et al., 2013). Thus, activation of indirect pathway neurons removes the tonic inhibition of GPe upon the GPi and STN, which further strengthens the inhibitory projections from the GPi and SNr upon the thalamus, providing a net inhibitory effect upon cortical activity overall (Cohen & Frank, 2009).

Recent evidence suggests that a third, "hyper-direct", pathway exists between the cerebral cortex and STN, in which direct excitatory projections from the neocortex synapse upon the STN and provide a global inhibitory response to the thalamus via the STN's excitatory projections to the GPi and SNr (Cohen & Frank, 2009; Redgrave et al., 2010). Global suppression via the hyper-direct pathway is observed early during response selection and is thought to be modulated by the degree of response conflict, such that actions with multiple competing responses elicit greater activation of the STN overall (Cohen & Frank, 2009). Computational neuroscientists hypothesize that the global suppression exerted by the STN and hyper-direct pathway afford the basal ganglia more time to both resolve the conflict between multiple competing responses and ensure that no action is selected prematurely (Frank, 2006).

Dopaminergic projections originating in the caudal SN (i.e. SNpc) play an important role in signaling within the basal ganglia and partially modulate activation within the direct and indirect pathways (Papoutsi et. al, 2014). Dopamine excites (i.e. activates) MSNs containing the D_1 receptor subtype, preferentially expressed within the direct pathway, while inhibiting MSNs that possess the D_2 receptor subtype, preferentially expressed within the indirect pathway. In both cases, activation of dopaminergic projections within the basal ganglia serves to disinhibit

thalamic feedback to the cortex, creating a net excitation effect overall (Cohen & Frank, 2009). In this way, dopamine acts as a focusing mechanism - enhancing the "signal" being broadcast among highly active excitatory D_1 cells while simultaneously decreasing the "noise" being emitted from less active inhibitory D_2 cells during action selection (Cohen & Frank, 2009).

In addition to facilitating action selection by differentially activating direct and indirect pathway MSNs, dopamine also plays a critical role in reinforcement learning and the acquisition of procedural tasks – processes that depend heavily upon the striatum (Cohen & Frank, 2009). Cortical regions associated with limbic (i.e. emotional), associative (i.e. cognitive) and sensorimotor function project largely segregated afferents to the striatum in a ventromedial to dorsolateral gradient (Redgrave et al., 2010). In-vivo electrophysiological recordings taken from behaving animals show that during skill learning, early acquisition depends heavily upon activation of MSNs within the dorsomedial (associative) striatum while late stage consolidation relies primarily on the activation of MSNs in the dorsolateral (sensorimotor) striatum (Yin et al., 2009). Activation of MSNs during each phase of a skill-learning task is pathway specific, such that acquisition relies heavily upon the activation of D_1 expressing striatonigral cells, while consolidation depends upon the activation of D_2 expressing striatopallidal cells (Yin et al., 2009). Thus, as a skill becomes more automatic and well engrained into procedural memory, the activity of direct pathway MSNs gradually subside while the activity of indirect pathway MSNs slowly increase.

Implicit learning depends on the presence and timing of dopamine release within the basal ganglia, which then serves to modulate MSNs that have already been activated by cortico-striatal glutamatergic input (Cohen & Frank, 2009). Specifically, phasic bursts of dopamine (i.e. ~100 ms latency; 100-200 ms duration) occur in response to unexpected rewards, and

dopaminergic firing drops below tonic baseline levels when a reward is expected but not received (Cohen & Frank, 2009; Redgrave, Gurney, & Reynolds, 2008). Thus, when a specific action is successful or rewarding, phasic bursts of dopamine facilitate long-term potentiation (LTP) within the already activated cortico-baso-thalamic circuit. In contrast, actions that fail to elicit reward or are deemed unsuccessful elicit tonic "dips" in dopamine levels which disinhibit indirect pathway MSNs (which are normally inhibited by dopamine via D_2 receptors), inducing LTP along the indirect pathway circuitry responsible for suppressing that action in the future (Cohen & Frank, 2009). In both cases, dopaminergic firing in the basal ganglia increases the likelihood of eliciting a successful response in response to the repeated presentation of a stimulus via Hebbian learning principles (Cohen & Frank, 2009).

Although the underlying mechanisms are not well understood, early neurodegeneration in HD tends to spare MSN within the direct pathway expressing D_1 receptors while MSN within the indirect pathway expressing D_2 receptors do not survive (Deng et al., 2004; Papoutsi et al., 2014). This raises the possibility that neurodegeneration occurring along the indirect pathway of the basal ganglia can cause the cognitive deficits observed during the pre-manifest and early stages of HD (Chen et al., 2013, Papoutsi et al., 2014). Dopamine receptor density is decreased in both pre-manifest and manifest HD (Chen et al., 2013), and neuroimaging studies suggest that a relationship between impaired dopamine receptor binding and the cognitive deficits observed in HD exists. Lawrence et al. (1998) used positron emission tomography (PET) to correlate the binding affinity of dopamine to D_1 and D_2 receptor subtypes with multiple cognitive tasks known to be sensitive to cortico-striatal function in HD. Results showed pre-manifest and manifest patients together were impaired on multiple cognitive tasks, and reduced binding affinity for D_2 receptor subtypes within the striatum was highly predictive of cognitive performance such that

patients who suffered the greatest impairments displayed the lowest levels of D_2 receptor binding affinity within the striatum. For a schematic of the gradient of pathology observed in the basal ganglia during the progression of HD, see Figure 2.

In addition to the effect that reduced dopamine receptor binding can have on cognitive performance, varying levels of dopamine within the striatum can also dramatically alter performance on basal ganglia dependent cognitive tasks. In HD, extracellular striatal dopamine levels display bi-phasic, time dependent changes such that levels increase during the early stage of the disease, and decrease at the later stages of the disease (Chen et. al., 2013). Patients of Parkinson's disease, which is caused by striatonigral (i.e. direct pathway) dopamine depletion in the dorsolateral striatum during the early stages of the disease and mesocorticolimbic/ventral depletion in the later stages, provide a unique opportunity to examine this relationship (Cools et al., 2001). Cools, Barker, Sahakian, and Robbins (2001) examined Parkinson's disease patients medicated with L-DOPA to investigate how dopamine systems contribute to cognitive performance in the domain of learning and attentional flexibility. After withdrawing L-DOPA medication, patients performed worse on a test of task-set switching known to depend on dorsolateral cortico-striatal circuits, while performance on a probabilistic reversal-learning task known to depend on orbitofrontal/ventral cortico-striatal circuitry improved. When L-DOPA was re-administered, the opposite pattern emerged. As the authors note, this is likely because administration of L-DOPA restored baseline levels of dopamine in the dorsolateral striatum (thus increasing performance on task-set switching), but "overdosed" the relatively intact orbitofrontal/ventral striatal circuitry (Cools et al., 2001).

Together, the evidence suggests that the timing of the cognitive declines observed during the early stages of HD may reflect the changes to the integrity of dopaminergic systems as well

as the topographical pattern of neurodegeneration observed as HD progresses (Papoutsi et al., 2014). Impaired signaling along the indirect pathway increases the tonic inhibition of the GPe upon the GPi and STN, which subsequently disinhibits thalamic feedback to the neocortex and allows competing responses to activate during action selection that would otherwise be suppressed (Papoutsi et al., 2014). At the same time, direct pathway MSNs become over activated in the presence of increased levels of extracellular glutamate, leading to even greater disinhibition of the thalamus overall. Dopamine's role in modulating action selection and learning amplifies during the early stages of the disease and diminishes throughout disease progression (Chen et al., 2013). Together, these deficits may manifest in perseveration, a classic symptom of HD that may be at the root of many of the cognitive deficits observed during the pre-manifest and early stages of the disease (Chen et. al., 2013; Giralt et al., 2012). As such, increased dopamine levels may "overdose" regions of the basal ganglia that remain relatively spared, while compromised D_2 receptor signaling in affected regions removes the ability to suppress competing response patterns. While bi-phasic changes in dopamine levels have been linked to movement symptoms (i.e. increased dopamine levels predict the onset of chorea during early HD and decreased levels predict akinesia during late HD), further studies tightly linking neuropathology with function will be necessary to connect these changes to cognition (Chen et al., 2013; Papoutsi et al., 2014).

As HD advances into the early and middle stages, a different cognitive profile begins to emerge. Deficits associated with the pre-manifest stage of HD continue to worsen, and impairments in episodic memory, spatial memory, and recognition memory begin to arise (Giralt et al., 2012; Montoya et al., 2006). While many attribute the deficits observed during manifest HD to the continued decline of cortico-striatal circuitry, this fails to incorporate the role of the

hippocampus and other related temporal lobe structures upon cognitive performance at this stage of the disease (Giralt et al., 2012). It is now widely accepted that there are multiple, competing memory systems that interact depending on the type of cognitive task being performed (Giralt et al. 2012; Gold, 2004; Hartley & Burgess, 2005). While implicit learning and non-declarative memory (i.e. procedural memory) depend largely upon activation of the striatum, spatial learning and declarative memory rely primarily upon the activation of the dorsal hippocampus (Hartley & Burgess, 2005; Poldrack et al., 2001).

A remarkable feature of the human brain is that it is plastic, and can reorganize neuronal circuitry to compensate for injury. In HD, functional imaging studies indicate that different brain regions such as the supplementary motor area, anterior cingulate, superior and inferior parietal lobe, premotor cortex, dorsolateral prefrontal cortex, and orbitofrontal cortex can play a compensatory role for striatal dysfunction depending upon the cognitive task being performed (Papoutsi et al., 2014). In pre-manifest HD patients, decreases in metabolic activity in brain regions such as the caudate, putamen, thalamus, insula, posterior cingulate, prefrontal cortex and occipital cortex occur simultaneously with increases in metabolic activity in the cerebellum, pons, hippocampus, and orbitofrontal cortex (Tang et al., 2013). Further, these shifts in metabolic activity become more pronounced over time, indicating a progressive compensatory network that is highly predictive of disease progression beyond volume loss alone (Tang et al., 2013). In manifest HD patients, Voermans et al. (2004) used fMRI to show that the hippocampus compensates for caudate dysfunction during a route-recognition task and patients maintain performance equal to that of healthy controls. As Papoutsi et al. (2014) note, individual differences that exist between patients in the ability to enlist compensatory mechanisms may

explain a great deal of the variability that exists between patients regarding the onset and progression of cognitive symptoms in HD.

A popular hypothesis links cognitive reserve (i.e. an individual's resilience against and ability to compensate for neurodegeneration) to sustained cognitive ability as HD progresses (Bonner-Jackson et al., 2013; Papoutsi et al., 2014). Papoutsi et al. (2014) posit that individuals possessing increased levels of cognitive reserve can process information more efficiently, and possess an increased ability to recruit new brain regions to compensate for a compromised neural network. Environmental enrichment (which increases cognitive stimulation and activity levels) delays onset of motor symptoms and slows the rate of cortical atrophy in a transgenic mouse model of HD (Hockly et al. 2002). Similarly, HD patients estimated to be closest to clinical onset possessing greater levels of cognitive reserve (as measured by a composite calculation of pre-morbid intellectual level, years of education, and occupational status) display slower rates of brain atrophy and cognitive decline compared to those with lower levels of cognitive reserve (Bonner-Jackson et al., 2013).

Though the relationship between cortical and striatal atrophy is likely to be complex, the cognitive phenotype observed during manifest HD likely reflects a combination of continued striatal atrophy, the spreading of neurodegeneration among cortical pyramidal cells, and the subsequent failure of compensatory neural mechanisms that preserve cognitive function (Giralt et al., 2012; Rosas et al., 2008, Papoutsi et al. 2014). Using magnetic resonance imaging (MRI), Rosas et al. (2003) showed that compared to controls, the most pronounced levels of atrophy in manifest HD patients occur in subcortical structures such as the caudate, putamen, globus pallidus, nucleus accumbens, and brainstem, although measureable cortical neurodegeneration is also observed in cerebral white matter, cerebral grey matter, and the hippocampus to a lesser

extent. Similarly, cross-sectional analysis of brain imaging measures in late stage manifest HD patients revealed increased cortical thinning within areas of the cingulate, pre-central, pre-frontal, occipital, parietal, and temporal cortices, accounting for as much as an 8.5% loss in volume compared to controls (Tabrizi et al., 2009). Further, cortical thinning predicts reduced performance on multiple tests of the UHDRS cognitive scale (a widely used measure of cognitive function in HD), including tasks such as Stroop Color Word Association, Symbol Digit Modalities, and Verbal Fluency (Rosas et al., 2008). The Verbal Fluency test is comprised of two variations, a phonetic version that depends on cortico-striatal circuitry, and a semantic version that depends on temporal lobe function (Baldo, Schwartz, Wilkens, & Dronkers, 2006). While manifest HD patients display deficiencies on both versions of the test, performance is impaired to greater extent on the phonetic version compared to the semantic version (Azmbujah, Haddad, Radanovic, Barbosa, & Mansur, 2007; Ho et al., 2002).

Together, the collective findings suggest that degeneration in HD begins in the basal ganglia, manifesting in abnormal cognitive processes known to depend on cortico-striatal circuitry (Giralt et al., 2012; Papoutsi et al., 2014). Throughout disease progression, atrophy within the basal ganglia becomes more severe and eventually progresses to the cortex, resulting in a failure of compensatory mechanisms and the appearance of deficits in new domains that depend less upon sub-cortical function and more upon the integrity of cortical structures (Giralt et al., 2012; Papoutsi et al., 2014). In the final stages of the disease, widespread failure of both sub-cortical and cortical systems leads to sub-cortical dementia and alterations in both simple and complex functions. Personality changes, decreased motivation, apathy, and depressive symptoms are commonly observed at this stage of the disease (Giralt et al., 2012).

Tabrizi et al. (2013) confirmed the overarching pattern of neurodegeneration seen in HD patients in a three-year longitudinal study of phenotypic progression known as TRACK-HD. Tabrizi and colleagues divided participants into one of four groups depending on the status of their diagnosis at baseline, using estimated years to onset and scores on total functional capacity (TFC) scale, which details level of function in the domains of workplace, finances, domestic chores, and activities of daily living. Groups were defined as PreHD-A (>10.8 years to predicted onset), PreHD-B (<10.8 years to predicted onset), HD1 (manifest with a total functional capacity score of 11-13), and HD2 (manifest with a total functional capacity score of 7-10). Results show that striatal volume is one of the most prominently recognizable clinical features among all subsets of patients, displaying a reduction in volume between 4.63% for PreHD-1 and 9.89% for HD2 over a three-year period (Tabrizi et al., 2013.) In contrast, grey matter volume remained relatively conserved compared to controls in the PreHD-A group (0.1% reduction of baseline volume), whereas manifest HD patients displayed a marked loss of grey matter over time, with as much as a 1.38% loss of volume compared to baseline. Interestingly, longitudinal changes in whole-brain atrophy, grey matter, white matter, caudate volumes, and impairments in emotional recognition were greater for pre-manifest patients who reached clinical diagnosis (i.e. were assigned a diagnostic confidence score of 4 on the UHDRS, signifying unequivocal presence of motor signs) during the study than those who did not. Whereas no association between neuropsychiatric symptoms such as affect, irritability, and apathy upon TFC exists for pre-manifest patients, these measures proved to be strong predictors of TFC decline for those with early-HD. As Tabrizi et al. (2013) note, increasing grey matter atrophy, especially in extrastriatal regions, correlates strongly with clinical onset and decline in TFC, signifying that

grey matter loss is a key marker of both clinical onset and disease progression and displays predictive power above and beyond CAG repeat length and age.

At the cellular level, the pathogenic hallmark of HD is cytoplasmic and intranuclear inclusions of aggregated mutant huntingtin protein (Walker, 2007). It is unclear whether the formation of aggregates is ultimately neuroprotective or harmful; some studies have shown that cells which contain aggregates, as opposed to soluble fragments of the mutated protein, survive longer than those which do not (Arresate, Mitra, Schweitzer, Segal, & Finkbeiner, 2004). Research links the mutant huntingtin protein (mHTT) to a multitude of abnormal cellular processes, including impaired proteasomal function, impeded intracellular vesicle and receptor trafficking, altered transcriptional regulation, and dysfunctional signaling among neurotrophic pathways that are critical for cellular survival (Harjes & Wanker, 2003; Li & Li, 2004).

Among the neurotrophic pathways that are altered in HD, many suggest that the brain derived neurotrophic factor (BDNF) signaling cascade plays a critical role in cellular degeneration and the manifestation of cognitive deficits (Li & Li, 2004; Milnerwood & Raymond, 2010). BDNF is a neurotrophin that is critical to cellular survival, and is particularly important for enhancing synaptic transmission, promoting synaptic growth, and facilitating synaptic plasticity (Lu, Nagappan, Guan, Nathan, & Wren, 2013). Reduced BDNF transmission remains a popular hypothesis because the huntingtin protein (HTT) modulates BDNF at the transcriptional level, and mHTT expression diminishes baseline levels of BDNF at many of the primary locations of pathophysiology associated with cognitive deficits in HD, including the striatum, neocortex, and hippocampus (Zuccato et al., 2001).

Striatal MSNs are unable to produce BDNF on their own, and instead must rely on other areas of the brain for its synthesis and delivery. Studies indicate that mHTT reduces both

anterograde and retrograde transport of vesicularized BDNF in vitro (Zala et al., 2008). Further, mHTT reduces retrograde transport of TrkB receptors, the primary receptor for BDNF, through its interaction with dynein, a motor protein essential for transport of cellular cargo along microtubules in axons (Liot et al., 2013). This raises the possibility that in HD, mHTT reduces BDNF supply to striatal neurons, and ultimately leads to neurodegeneration (Li & Li, 2004). Interestingly, genetically reducing the amount of mHTT expressed in cortical efferents improves electrophysiological and behavioral phenotypes in mice, supporting the hypothesis that mHTT alters cortical communication with their striatal targets by either impeding the delivery of critical trophic factors (e.g. BDNF) or disrupting the synchronicity of communication between cells at the network level (Estrada-Sanchez et al., 2015). The BDNF hypothesis remains controversial, however, since other studies suggest that increased activation of the p75 neurotrophic receptor ($p75_{NTR}$), a non-selective nerve growth factor receptor, may account for the reduced synaptic plasticity observed in HD (Plotkin, et al, 2014). Whereas activation of TrkB receptors by BDNF promote neuronal survival, axonal outgrowth, and synaptic plasticity (i.e. LTP), activation of $p75_{NTR}$ facilitates cell death, inhibits axonal outgrowth, and is necessary for long-term depression (Chapleu & Pozzo-Miller, 2012). Plotkin et al. (2014) failed to find altered striatal BDNF and TrkB mRNA in two mouse models of HD, suggesting impairment in BDNF plasticity must occur downstream of TrkB receptor binding. When $p75_{NTR}$ receptors were knocked-down or inactivated, Plotkin et al. (2014) completely restored any synaptic LTP deficits previously observed. It is interesting to note that $p75_{NTR}$ can be activated by a number of ligands, including BDNF itself, raising the possibility that in HD BDNF is both activating and inhibiting LTP through its interaction with TrkB receptors and $p75_{NTR}$ (Plotkin & Surmeier, 2014).

Importantly, synaptic pathophysiology occurs prior to cell death in both humans and animal models of the disease (Milnerwood et al., 2006; Orth et al., 2010). Morphological changes are observed in the dendrites of MSNs in human HD patients, and a reduced number of dendritic spines are found in the MSNs in animal models of the disease (Smith, Brunden, & Lee, 2005). The finding that synaptic dysfunction in HD occurs prior to cell death is paramount, because it opens new avenues in regards to potential therapeutic interventions. In that regard, it may be possible to reverse the effects of neurite loss and overall synaptic failure using drug therapy as long as the disease were diagnosed early enough in its progression (i.e. before cell death occurs).

Mouse models are the most useful and practical tool to test potential therapies because they possess a homologous huntingtin gene (Hdh) that is roughly 91% identical to that of humans, and share many physiological and anatomical traits with humans (Barnes et al. 1994; Ehrnhoefer, Butland, Pouladi, & Hayden, 2009). Though other animal models of HD exist (e.g. *C. elegans*, *Drosophila*, sheep, pigs, and monkeys), these models either fail to exhibit the behavioral complexity necessary to study complicated processes such as cognition, or incur many practical, financial, and ethical issues (Ehrnhoefer et al., 2009). Thus, mouse models strike an important balance necessary to conduct research efficiently and practically. Since a single genetic mutation is responsible for the pathogenesis observed in HD, several mouse models have been engineered to recapitulate the features of the disease seen in humans, although each differs in the manner that it is created and is distinguished by a unique set of strengths and weaknesses. At the present, three main types of genetically engineered mouse models exist: N-terminal transgenic, full-length transgenic and knock-in models (Menalled & Chesselet, 2002). Homozygous knock-out mice (i.e. completely inactivating the huntingtin gene) were created first

but animals created in this fashion fail to recapitulate the symptoms associated with human HD and die during embryonic development (Duyao et al., 1995). Apart from identifying an important role for the huntingtin protein during embryogenesis (Duyao et al., 1995), this suggests that the pathology caused by the HD mutation is not due to loss of function alone (Duyao et al., 1995, Menalled & Chesselet, 2002), and is more likely due to a combination gain of function and loss of function mechanisms together (Menalled & Chesellet, 2002).

The first mouse model of HD to be created was an N-terminal fragment model, which was constructed by randomly inserting exon 1 of the mutated human huntingtin gene into the mouse genome via pronuclear injection. Thus, N-terminal fragment mice express the mutated human gene in addition to two endogenous copies of the murine gene (Menalled, et al., 2014). This process is very disruptive to the mouse genome; inserting the affected human huntingtin gene has deleterious effects on mouse chromosomal DNA near the interaction site and can potentially introduce additional abnormalities on top of those caused by the mutant human huntingtin gene (Menalled et al., 2014). The phenotype associated with N- terminal models is severe and rapid, a product of the fact that similar to humans, soluble N-terminal fragments of mHTT are more toxic than the full-length protein (Arresate et al., 2004). The rapid disease progression associated with N-terminal transgenic model makes them among the cheapest to house and quickest to display pathological signs, making them the most popular model to use in pre-clinical research. A review of pre-clinical trials conducted by Menalled and Brunner (2014) found that over half of the studies conducted utilized N-terminal fragment mice for their study. However, the rapid progression associated with the model also presents a disadvantage in that it is impossible to sequence the phenotypic progression of the disease, thus hampering the ability of researchers to measure deficits that characterize the pre-manifest stage of the disease.

Full-length transgenic models of HD differ from N-terminal models in that a full-length copy of the mutated human gene is inserted into the mouse genome via a yeast or bacteria artificial chromosome (Menalled et al., 2014). The reduced toxicity associated with the insertion of the full length gene results in a slower and more gradual expression of the disease phenotype in the mouse (Menalled et al., 2014), making it possible to clearly establish deficits which belong to the pre-manifest stage of the disease. Issues with this model are still apparent, however, as full-length transgenic mice tend to gain weight compared to other models and healthy controls, a phenomenon that is uncharacteristic of human HD patients who instead display impaired energy metabolism and reduced body weight (Menalled et al., 2014). Weight gain can confound results in experiments which the mice must utilize motor function to complete the task, ultimately affecting both tests designed to measure motor function (e.g. rotarod) and cognition (e.g. Morris water maze).

Unlike transgenic models, knock-in models (KI) are created by altering the length of the CAG tract in the homologous mouse huntingtin gene in embryonic stem cells (Menalled et al., 2014), resulting in a number of advantages compared to other HD mice. KI mice can be either homozygous or heterozygous for the *Hdh* gene; those expressing one mutant allele as well as one wild-type allele allow for proper gene dosage compared to the transgenic lines and are a more accurate depiction of the human condition (Menalled et al., 2014). KI mice are also a more precise representation of the human condition because the manipulation of mouse *Hdh* gene allows the endogenous murine promoter to control levels of gene expression (Menalled, 2005). Phenotypic expression KI mice most closely mimic that of humans, where initial abnormalities are very mild and closely resemble the pre-symptomatic stage of the disease. For this reason, KI mice are among the highest in construct validity and one of the most useful tools to measure pre-

symptomatic deficits such as cognition (Menalled, 2005). At later stages, knock-in mice develop overt behavioral phenotypes including motor abnormalities (Menalled et al., 2014). KI mice, and their relatively subtle phenotypes compared to other models do present a disadvantage in that it is difficult to measure phenotypic abnormalities reliably. For this reason, Menalled and Brunner (2014) found in their review of pre-clinical trials that only 3% of the studies reviewed utilized knock-in models for their studies.

Many therapies have been successful in animal models of HD, only to fail when tested in humans (Menalled & Brunner, 2014). Multiple explanations exist, ranging from the lack of robustness in pre-clinical studies to the misuse of statistical analysis methods (Menalled & Brunner, 2014). Ioannidis (2005) suggests that the majority of studies published in the field of biomedical research are actually false, noting several tendencies characteristic of the field such, as bias in experimental design (i.e. selective reporting of findings or post-hoc analyses of unspecified hypotheses), testing of the same research question by several independent research teams, utilization of small sample sizes to streamline experiments, and the use of outcome measures that are not universally agreed upon all greatly reduce the likelihood that a published research finding is actually true. Further, Button et al. (2013) conducted a meta-analysis suggesting that studies in the field of neuroscience achieve on average only 21% statistical power across the field and state that the reduced power observed in these studies also reduce the likelihood that a statistically significant finding actually reflects a true effect. That is, the authors argue that for an underpowered study to achieve a nominally statistically significant result, the measured effect size must be inflated beyond the point that is truly reflected in the population, a phenomenon known as the winner's curse (Button et al., 2013). Taken together, these findings

suggest that therapies that have been successful in animal models may have ultimately failed in humans because the original research findings may have been spurious from the outset.

Another possible explanation for the lack of translatable therapeutic research in HD may be that experimenters tend to select improper animal models and use poor behavioral endpoints to test potential therapies. For example, Menalled and Brunner (2014) found in a meta-analysis of pre-clinical HD studies that only 5% of experimenters utilized cognitive endpoints and often relied on measures such as motor ability, survival rate, and neuropathology to determine treatment efficacy instead. It can be argued that behavior represents the final output of the brain, so it should follow that use of KI models as well as endpoint measures that focus on behavioral output such as cognition, especially those that arise during the pre-manifest stage before cell death occurs, will improve the translation of therapies from animals to humans.

Of the knock-in mouse models of HD, relatively little behavioral characterization has been conducted on the B6.$Htt^{Q111/+}$ KI mouse model of HD thus far. $Htt^{Q111/+}$ mice are part of an allelic series of KI mice created by Vanessa Wheeler and Marcy MacDonald at Massachusetts General Hospital consisting of 18, 48, 78, and 90 CAG repeats, and mimic the genetics of human HD by including 109 CAG repeats in the endogenous murine gene (Menalled et al., 2014; Wheeler et al., 1999). Although initially created on a mixed 129SvEv/CD1 genetic background (Wheeler et al., 1999), $Htt^{Q111/+}$ mice and the other KI models in this allelic series are now maintained on a C57BL/6J inbred background to reduce variability and allow researchers to investigate the influence of CAG size on desired outcome measures (Menalled et al., 2014). The majority of behavioral characterization associated with this model suggests mild and late onset behavioral phenotypes (Menalled, 2005). Hölter et al. (2013) conducted the most comprehensive behavioral characterization of $Htt^{Q111/+}$ mice to date, finding that heterozygous mice display

impairments in social discrimination learning at three months, motor learning at six months, olfactory discrimination between six and eight months, decreased anxiety-like phenotype and distance traveled in the open field at nine months, and motor deficits at ten and a half months of age. Both recognition deficits and long-term memory deficits on a novel object recognition and object relocation task have been observed at six months of age (Brito et al., 2014), as well as spatial memory deficits on Morris water maze probe trials at eight months of age (Giralt et al., 2011). Further, working memory and reversal learning deficits are observed on a delayed matching to position (DMTP) and delayed non-matching to position (DNMTP) task at eight months of age (Yhnell, Dunnett, & Brooks, 2015).

This thesis will continue to characterize the behavioral phenotype associated with the $Htt^{Q111/+}$ mouse model of HD by attempting to replicate the findings obtained in previous experiments and probing for novel behavioral phenotypes characteristic of the pre-manifest stage of the disease that depend on the striatum. $Htt^{Q111/+}$ mice were subjected to three assays meant to probe different aspects of cognitive and psychiatric function. The two-cue Morris water maze, developed by Lee, Duman, and Pittinger (2008), depends on dorsolateral striatal function and measures procedural learning and memory ability that is impaired during the pre-manifest stage of HD. The open field test provides an index of anxiety-like phenotype and spontaneous locomotor activity, and measures HD related psychiatric symptoms. Lastly, the object location task depends on hippocampal function and probes spatial long-term memory deficits that emerge during the manifest stage of HD. We hypothesize that the results obtained from a large cohort of nine month old $Htt^{Q111/+}$ mice will provide a cross-sectional snapshot of cognitive ability, thus making both the $Htt^{Q111/+}$ mouse model and subsequent behavioral assays a suitable option for pre-clinical trials aiming to test novel therapeutics during the pre-manifest stage of HD.

Methods

Ethical Considerations

All procedures involving the use of experimental animals were approved by the Western Washington University Institutional Animal Care and Use Committee and were in accordance with the *Guide for the Care and Use of Laboratory Animals* described by the National Institutes of Health.

Experimental Animals

Experimental animals consisted of sixty-one female C57BL/6J mice. Of these, 32 mice were $Htt^{Q111/+}$ heterozygous mutant mice, and 29 were $Htt^{+/+}$ counterparts used as controls. Mice were housed under reverse light/dark cycle conditions (12:00 pm – 12:00 am dark cycle) and were provided access to food and water ad-libitum. All testing was conducted between 1:00 pm and 9:30 pm, during the active phase of the experimental animals.

Materials and Procedure

Two-cue Morris water maze.

Procedural learning was assessed using a two-cue Morris water maze (MWM) task adapted from the procedure used by Lee et al. (2008). The MWM apparatus consisted of a circular pool (125 cm diameter; water depth of 51.5 cm) filled with room temperature water made opaque with the addition of white, non-toxic latex paint. Four positions outside the maze were arbitrarily designated as north (N), south (S), east (E), and west (W) to provide starting locations and to divide the maze into four quadrants: NW, SW, NE, & SE. Testing consisted of four sub-components: shaping, one-cue training, two-cue training and probe trials. For all phases of the experiment, animals were moved into the water-maze room and allowed to habituate for 30 minutes prior to testing.

Shaping and one-cue training.

At four and a half months of age, each experimental animal was exposed to the task for three consecutive days. Day one consisted of shaping. Each mouse was placed upon a black platform made of acrylic plastic (12x12 cm) located 1 cm below the surface of the water and marked with a neutral grey cue (5 cm diameter, 11 cm high). During shaping, animals were permitted to rest upon the platform for 30 seconds before being returned to their home cage. Any experimental animal that left the platform before meeting the 30 second criteria was gently guided back to the platform a maximum of two times, after which the trial was terminated and the animal was returned to its home cage. This procedure was repeated four times total for each mouse. Platform location for each trial was pseudorandomized such that every mouse was exposed to each quadrant once, with an inter-trial interval of approximately 30 minutes.

Following shaping, days two and three consisted of one-cue training. Once again the escape platform was marked with the neutral grey cue, and placed in the center of one quadrant (i.e. NW, SW, NE, or SE). For each trial, mice were placed in the water facing toward the wall at a point opposite from the escape platform (i.e. if the escape platform were located in the NW quadrant, entry location could be either south or east). Mice were permitted to search for the platform for a maximum of 120 seconds; if a mouse did not find the platform in the allotted time, they were gently guided toward the escape platform a maximum of two times before the trial was terminated and they were returned to their home cage. Upon finding the platform, mice were permitted to rest for 15 seconds. If a mouse failed to reach the 15 second criteria, they were gently guided back toward the platform a maximum of two times. Mice that left the platform more than two times total were returned to their home cage, and the training trial was terminated. As with shaping, this procedure was repeated four times total for each mouse, and platform

location was pseudorandomized between trials such that every mouse was exposed to each quadrant once, with an inter-trial interval of approximately 30 minutes.

Two-cue training and probe trials.

At nine months of age, experimental animals were tested on the two-cue version of the MWM for seven days, consisting of four trials per day and with a 45-minute inter-trial interval between each trial. During two-cue training trials, a goal cue was marked with one of two distinct visual cues (5 cm diameter, 11cm high; painted with either horizontal or vertical black and white stripes), and an escape platform made of white acrylic plastic (15 cm diameter) was placed in the center of a quadrant 1 cm below water level. The remaining visual cue (i.e. the lure cue) was placed in a quadrant adjacent to the goal cue and did not permit the animal to escape, but was visually identical to the goal cue except for the pattern. Goal cue and lure cue patterns were counterbalanced between mice, and held constant throughout the duration of the two-cue phase (i.e. for each mouse, goal cue and lure cure pattern remained the same across all trials). In this way, experimental animals were forced to associate one of the visual patterns with escape from the maze. To further reinforce the use of visual pattern as a means of escape, the goal cue was never placed in the same location twice in a row, and the relationship of the lure cue to the goal cue (i.e. left or right, depending on starting location) was never the same more than twice in a row. In all, eight orientations of goal cue, lure cue, and starting location were possible. Each animal was pseudorandomly exposed to each orientation once for every two days of training. For a schematic of all possible MWM orientations, see Figure 3.

For each two-cue training trial, mice were placed into the maze at the pre-determined starting location facing toward the wall, and were permitted to search for the escape platform for a maximum of 120 seconds. Mice who successfully reached the escape platform were permitted

to rest for 15 seconds before being returned to their home cage. If an animal successfully navigated to the escape platform but left before reaching the 15 second criteria, the trial continued until the mouse returned to the escape platform for 15 continuous seconds or a maximum trial of 120 seconds was reached.

During the fourth trial of days three, five, and seven, a probe trial was administered to assess procedural memory. The orientation for probe trials was determined in the same manner as two-cue training trials, but the escape platform was removed to make escape impossible. Probe trials began by placing the mouse into the maze at the pre-determined starting location facing toward the wall, after which mice were permitted to swim freely for 60 seconds. After the 60 second probe trial had elapsed, mice were removed from the water-maze and returned to their home cage.

During both two-cue training trials and probe trials, the swim pattern of each mouse was recorded using an overhead camera. Swim patterns were subsequently analyzed using Noldus Ethovision XT 8 (Noldus, Spink, & Tegelenbosch, 2001). For two-cue training trials, the primary outcome measure was the latency to reach the escape platform during each two-minute trial. For probe trials, procedural memory was interpreted as a bias for swimming in the quadrant containing the goal cue relative to quadrant containing the lure. To eliminate nuisance variables (i.e. the time spent swimming in quadrants containing neither the goal or the lure), time spent in the goal quadrant was calculated as a percentage of the total time spent in both the goal and lure quadrant, using the formula: Goal Preference = Goal Occupancy/ (Goal Occupancy+Lure Occupancy). The proportion of time spent in the goal quadrant relative to the lure quadrant (i.e. the goal preference), and the change in goal versus lure quadrant preference over each day of probe trials was then compared between genotypes. Mice were considered to

have intact procedural memory if they displayed a preference for the goal quadrant relative to the lure quadrant during probe trials.

Open field.

Immediately following two-cue MWM testing, nine month old mice were subjected to the open field test, which assesses anxiety levels, exploratory behavior, and spontaneous locomotor activity, during the habituation phase of the object location task (OLT), described below. Days one and two of the OLT each consisted of habituation to a novel arena, which was constructed of a white acrylic plastic floor measuring 44x44 cm, with black acrylic plastic walls measuring 44 cm high. On both days one and two, mice were placed in the arena in the absence of any objects and were permitted to explore freely for 10 minutes. Between trials, the floor and walls of the arena were cleaned thoroughly using 70% EtOH. During open field testing, activity was recorded using an overhead camera, and open-field behavior obtained during day one was analyzed using Noldus Ethovision XT 8 (Noldus, Spink, & Tegelenbosch, 2001).

The primary behavioral measures obtained during the open field task included total ambulation (i.e. total distance traveled), the amount of time spent actively exploring the arena, average velocity, thigmotaxis (i.e. time spent along the walls compared to the center of the arena), which is believed to measure of anxiety levels in mice (Simon, Dupuis, & Costentin, 1994). Average velocity was calculated by dividing the total distance traveled by the amount of time that mice spent actively exploring the arena. Thigmotaxis levels were assessed by creating three concentric zones inside the open field arena: an outer zone, an intermediate zone, and an inner zone. To eliminate nuisance variables (i.e. the time spent in the intermediate zone), the time spent along the wall of the arena was expressed as a percentage of the total time spent in both the inner zone and the outer zone using the formula: Wall Preference = Outer Zone

Occupancy/ (Outer Zone Occupancy+Inner Zone Occupancy). Scores were compared between genotypes, and mice were considered less anxious if they spent more time in the center of the arena (Figure 4a) than against the wall (Figure 4b).

Object location task.

Following open field testing on days one and two, nine month old mice were tested on the object location task (OLT), which probes spatial long-term memory and is known to depend upon the function of hippocampus (Murai, Okuda, Tanaka, & Ohta, 2006). On day three, mice were subjected to the acquisition phase of the object OLT. Four sets of identical objects were used: Erlenmeyer flasks, terra cotta pots, Nalgene bottles filled with blue food coloring, or Nalgene bottles covered with textured coozies. Pilot testing was conducted prior to ensure that no one object was more appealing to the mice than another, and all objects were counterbalanced between experimental animals to ensure equal representation. Large intra-maze cues (a square, a triangle, an equal sign, and a plus) were taped to the walls of the arena along the north, south, west and east wall respectively, since research has indicated that visual depravation of spatial cues can obscure results (Murai et al., 2006). Mice were placed into the apparatus such that they were facing two identical objects (i.e. facing north) placed in the NW and NE corners of the arena, and were permitted to explore for 10 minutes. Following each trial, the apparatus and objects were cleaned thoroughly with 70% EtOH, and mice were placed back in their home cage and returned to the vivarium to rest for 24 hours.

On day four, mice were tested on the relocation phase of the OLT. During relocation, one of the two identical objects placed in the NW or NE corner of the arena was relocated to the diametrically opposite corner of the arena (i.e. if the NW object was relocated, it was placed in the SW corner; if the NE object was relocated it was moved to the SE corner). The object that

was relocated (i.e. the object to the left or the right) was counterbalanced between experimental animals. During the relocation phase, mice were placed into the arena facing north and permitted to explore the objects for five minutes. Following each trial, the apparatus and objects were cleaned using 70% EtOH and experimental animals were returned to their home cage. The primary outcome measure was the number of explorations toward each object, defined as any event where the mouse interacted with the object or oriented its head toward the object such that its nose was within 2 cm proximity. The total number of explorations to the relocated object was then expressed as a percentage of total explorations using the equation: Novel Preference = Novel Events/ (Novel Events+Familiar Events). These data were compared between genotypes, and spatial long-term memory was determined to be intact if the animal displayed a preference for the relocated object compared to the familiar object. To determine if there was a reduction in motivation to explore the objects, the total number of explorations toward both objects was also compared between genotypes.

Statistical Analyses

All data were analyzed using the R statistical computing software (R Core Team, 2015). Two-cue MWM training trials and probe trials were analyzed using a repeated measures linear mixed effects analysis of variance (ANOVA), which allows for both fixed and random effects. In these analyses, genotype was treated as a fixed effect and subject specific rates of change over time (i.e. individual differences between mice not due to the effect of genotype) were treated as random effects. Post-hoc analyses examining the effect of time, or the effect of genotype over time were analyzed using the Ryan-Einot-Gabriel-Welsh (REGWQ) q test in order to maintain the familywise error rate for each pairwise comparison at an alpha level of .05. Total ambulation, active exploration time, average velocity, preference for the outer zone of the open

field, number of total explorations, and the proportion of explorations toward the relocated object were analyzed using independent samples t-tests for the open field test and OLT, respectively. Paired samples t-tests were used to determine relocated object preference for each genotype during the OLT.

Results

Two-cue Morris water maze

Two-cue Morris water maze training trials.

The latency to reach the escape platform during two-cue training trials was analyzed using a 2x7 (Genotype x Day) linear mixed effects ANOVA. There was a main effect of day such that the latency to reach the escape platform varied for all mice depending on the day of testing, $F(6,354) = 62.74$, $p < .001$, $\eta_p^2 = .50$. REGWQ post-hoc comparisons suggested that there was a statistically significant reduction in the average latency to reach the escape platform for all mice between day one and days two, three, four, five, six, and seven. In addition, the average latency to reach the escape platform for all mice on day two was statistically significantly different from the latencies to reach the escape platform on days four, five, six, and seven. No other differences were statistically significant. There was no main effect of genotype, $F(1,59) = 0.49$, $p = .49$, $\eta_p^2 = .002$ and no genotype by day interaction, $F(6,354) = 0.14$, $p = .99$, $\eta_p^2 = .003$, suggesting that all mice had acquired a strategy for locating the escape platform by day 2 of two-cue training, and that $Htt^{Q111/+}$ and $Htt^{+/+}$ mice acquired an escape strategy at similar rates (Table 1; Figure 5).

Two-cue Morris water maze probe trials.

The percentage of the total time spent in the goal and lure quadrant, and the change in quadrant preference during each day of two-cue probe trials were compared between genotypes

using a 2x2x3 (Genotype x Quadrant x Day) linear mixed effects ANOVA. Since the percentage of time spent in the goal and lure quadrant did not vary as a function of genotype or day (i.e. the total percentage of time spent in the goal and lure quadrant was always 100%) the main effects and interaction between these variables canceled out and were not considered in any subsequent analyses. There was a main effect of quadrant such that the goal quadrant (M = .52, SD = .11) was preferred on average over the three days of probe trials relative to the lure quadrant (M = .48, SD = .11), $F(1,175) = 12.74$, $p < .001$, $\eta_p^2 = .04$. However, the main effect of quadrant was qualified by an interaction between genotype and quadrant, $F(1,175) = 4.85$, $p = .03$, $\eta_p^2 = .01$, indicating that goal cue preference differed depending on genotype. A test of simple main effects revealed that $Htt^{Q111/+}$ mice displayed a statistically significant preference for the goal quadrant on average over the three days of probe trials (M_{goal} = .53, SD = .12; $t(95) = 2.90$, $p <$ .01, $d = 0.50$), while $Htt^{+/+}$ mice showed no preference for the goal quadrant overall (M_{goal} = .51, SD = .11; $t(84) = 0.61$, p =.54, $d = 0.18$). There was no quadrant by day interaction, $F(2,175) =$ 0.35, $p = .71$, $\eta_p^2 = .002$, or genotype by quadrant by day interaction, $F(2,175) = 0.18$, $p = .83$, $\eta_p^2 = .001$. Altogether, these results suggest that $Htt^{Q111/+}$ mice established a preference for the goal cue by day 3 that remained throughout the duration of testing while $Htt^{+/+}$ mice displayed no preference for either the goal cue or the lure cue during any of the three days of probe trials, indicating improved procedural memory ability in $Htt^{Q111/+}$ mice (Figure 6).

Open field

To examine differences in exploratory behaviors and anxiety levels during the open field session between genotypes, a series of independent samples t-tests on outcome measures such as total exploratory activity, overall time spent actively exploring the arena, average velocity, and levels of thigmotaxis were conducted. There was a statistically significant reduction in the

overall activity levels observed in $Htt^{Q111/+}$ mice ($M_{distance}$ = 3547.39 cm, SD = 595.06) compared to $Htt^{+/+}$ mice ($M_{distance}$ = 4003.78 cm, SD = 781.56), $t(59) = 2.58$, $p = .01$, $d = 0.66$, indicating that $Htt^{Q111/+}$ mice were hypoactive compared to $Htt^{+/+}$ during the open field session (Figure 7). Despite traveling less overall, no differences were observed between $Htt^{Q111/+}$ mice ($M_{exploration}$ = 417.16 sec, SD = 46.47) and $Htt^{+/+}$ mice ($M_{exploration}$ = 440.51 sec, SD = 47.12) in the amount of time mice spent actively exploring the open field arena, $t(59) = 1.95$, $p = .06$, $d = 0.50$, although this comparison did approach statistical significance (Figure 8). The average velocity of $Htt^{Q111/+}$ mice ($M_{velocity}$ = 8.49 cm/s, SD = 0.86) was statistically significantly reduced compared to $Htt^{+/+}$ mice ($M_{velocity}$ = 9.02 cm/s, SD = 1.05), $t(59) = 2.18$, $p = .03$, $d = 0.56$ (Figure 9). Lastly, a statistically significant difference was found between $Htt^{Q111/+}$ mice (M_{wall} = .90, SD = .07) and $Htt^{+/+}$ mice (M_{wall} = .86, SD = .07), such that $Htt^{Q111/+}$ mice displayed increased levels of thigmotaxis and spent more time along the wall during the open field session, $t(59) = -2.10$), $p = .04$, $d = 0.54$, indicating increased anxiety levels in $Htt^{Q111/+}$ mice (Figure 10). Overall, these results suggest that a decreased motivation to explore, subtle motor deficit, or increased anxiety levels may contribute to the hypoactivity observed in $Htt^{Q111/+}$ mice during open field exploration.

Object Location Task

Paired samples t-tests were used to assess the preference for the relocated object relative to the familiar object for each genotype, and independent samples t-tests were used to assess relocated object preference and overall exploratory activity between genotypes. Both $Htt^{Q111/+}$ mice ($M_{relocated}$ = .55, SD = .12; $t(31) = 2.60$, $p = .01$, $d = 0.83$) and $Htt^{+/+}$ mice ($M_{relocated}$ = .60, SD = .12; $t(27) = 4.41$, $p < .001$, $d = 1.67$) displayed a statistically significant preference for the relocated object compared to the relocated object, indicating intact spatial long term memory for

both genotypes. Further, there was no statistically significant difference between genotypes in their preference for the relocated object, $t(58) = 1.41$, $p = .17$, $d = 0.36$, suggesting that spatial long term memory was not impaired in $Htt^{Q111/+}$ mice relative to $Htt^{+/+}$ mice overall (Figure 11). Interestingly, there was a statistically significant reduction in the number of total explorations toward both objects by $Htt^{Q111/+}$ mice ($M_{explorations} = 24.00$, $SD = 7.34$) relative to $Htt^{+/+}$ mice ($M_{explorations} = 28.50$, $SD = 6.50$), $t(58) = 2.50$, $p = .02$, $d = 0.64$, suggesting that $Htt^{Q111/+}$ mice displayed a reduction in exploratory behavior similar to the one observed during open field exploration (Figure 12). Altogether, these results indicate that spatial long term memory remains intact in $Htt^{Q111/+}$ mice, although a hypoactive phenotype potentially stemming from a decreased motivational drive to explore, a neophobic response to novelty, a subtle motor deficit, or increased anxiety levels leads to a reduction in the total number of explorations toward both objects in $Htt^{Q111/+}$ mice overall.

Discussion

This thesis aimed to continue the behavioral characterization of the $Htt^{Q111/+}$ KI mouse model of HD, with the intent of discovering novel deficits characteristic of the pre-manifest stage of the disease suitable for use in pre-clinical trials. A number of interesting phenotypes were uncovered in this study, including improved procedural memory relative to $Htt^{+/+}$ mice during two-cue MWM probe trials, hypoactivity, reduced velocity, and increased anxiety levels during open field exploration, and a reduction in the total number of explorations toward both objects during the OLT.

During two-cue MWM training trials, $Htt^{Q111/+}$ and $Htt^{+/+}$ mice did not differ in the rate which an escape strategy was acquired over the seven days of testing. Specifically, both $Htt^{Q111/+}$ and $Htt^{+/+}$ mice acquired an escape strategy by day two that held constant for the

remainder of two-cue MWM training trials. Previous literature suggests that task acquisition ability varies in $Htt^{Q111/+}$ mice depending on the experimental assay being administered as well as the underlying cognitive ability that is being probed. $Htt^{Q111/+}$ mice display normal rates of task acquisition but impaired memory consolidation during probe trials on a MWM task measuring spatial LTM ability (Giralt et al., 2011), while task acquisition and reversal learning are impaired in a delayed matching to position (DMTP) and delayed non-matching to position (DNMTP) operant task designed to measure working memory ability (Yhnell, et al., 2015). The results obtained in this study ultimately indicate that acquisition of a procedural learning task was not impaired in $Htt^{Q111/+}$ mice compared to $Htt^{+/+}$ counterparts during two-cue MWM training trials.

Further evidence supporting this claim stems from the original experiment from which the two-cue MWM task was adapted. To show that two-cue MWM performance depends on striatal function, Lee et al. (2008) compared the performance of healthy wild-type (WT) mice to mice in two experimental conditions. In the first group, Lee et al. (2008) introduced extreme striatal insults in experimental mice by lesioning a large portion of the dorsolateral striatum. In the second group, the authors utilized a much milder model of striatal dysfunction in KCREB mutant mice, which possess specific deficits in procedural learning due to localized inhibition of the cAMP response element-binding protein (CREB) family of transcription factors in the dorsolateral striatum that are critical for LTM consolidation (Pittenger et al., 2006). While the mice with widespread dorsostriatal lesions were impaired during the acquisition phase of the two-cue MWM, KCREB mutant mice with mild striatal dysfunction acquired the task at a rate similar to WT mice (Lee et al., 2008). Similar to KCREB mutant mice, phospho-CREB levels (i.e. the transcriptionally active form of CREB) are reduced in the cortex of $Htt^{Q111/+}$ mice

beginning at five months of age (Gines et al., 2003). It is reasonable to assume that the performance of $Htt^{Q111/+}$ mice would more closely resemble the level of KCREB mutant mice than the more severely impaired mice with widespread dorsolateral striatal lesions. Given that the two-cue MWM protocol was unable to detect acquisition deficits in a mild model of corticostriatal dysfunction in the study it was originally derived from (Lee et al., 2008; Pittinger et al., 2008), the lack of differences observed between genotypes during two-cue training in this study likely reflects the relatively subtle phenotype associated with $Htt^{Q111/+}$ mice.

Interestingly, $Htt^{Q111/+}$ mice outperformed $Htt^{+/+}$ mice during two-cue probe trials and displayed a greater affinity for the goal-cue relative to the lure-cue over the three days of testing, which indicates that $Htt^{Q111/+}$ mice display improved procedural memory consolidation compared to $Htt^{+/+}$ counterparts at nine months of age. Although these findings do not align with the original hypotheses of the study, prior research suggests that the same mechanisms contributing to neurodegeneration in HD can also enhance some forms of learning in parallel by simultaneously amplifying neural plasticity in pre-symptomatic HD patients (Beste, Wascher, Dinse, & Saft, 2012). Glutamatergic neurotransmission at NMDA receptors plays an important role in both memory consolidation and excitotoxic cell death (Beste et al., 2012). In that regard, NMDA receptor activation causes an influx of Ca^{2+} into the postsynaptic neuron, which then acts as an important second messenger that can either facilitate synaptic LTP (Malenka & Nicoll, 1999) or trigger apoptosis via caspase activation (Andre, Cepeda, and Levine, 2010) depending upon its concentration levels inside the cell. Similar to the biphasic changes in dopamine levels observed throughout the progression of HD (i.e. increased levels during the early stages followed by decreased levels in the later stages) glutamate levels in the striatum are found to be increased during the early stages and decreased during the later stages in animal models of the disease

(Andre et al., 2010). Additionally, energy metabolism deficits elicited by mHTT can cause both AMPA and NMDA receptors to become overly sensitive and more readily activated by endogenous levels of glutamate (Beal & Ferrante, 2004). Together, this suggests that HD mice could potentially perform better than $Htt^{+/+}$ mice during two-cue probe trials if the neuropathological changes occurring in the striatum of nine month old $Htt^{Q111/+}$ mice were to cause an increase in glutamatergic transmission that facilitates LTP and not widespread excitotoxic cell death. In order to validate this claim, however, further studies linking neuropathology to cognitive function will be necessary.

Perhaps a more parsimonious explanation for the results obtained during two-cue probe trials is that the task simply did not work as anticipated. Though $Htt^{Q111/+}$ mice displayed a statistically significant preference for the goal cue on average over the three days of two-cue probe trials, small effect sizes and the lack of a robust preference for the goal cue call into question the practical significance of this finding. Furthermore, $Htt^{+/+}$ mice never established a goal cue preference at any point over the course of two-cue probe trials, which likely signifies that the procedure was not able to measure the construct of procedural memory effectively. Lee et al. (2008) contend that a degree of extinction can occur during two-cue probe trials after mice discover that the platform is no longer present and escape is not possible, and argue that it is possible for this effect to obscure the results of the experiment. From an observational standpoint, mice seemed to swim arbitrarily between the two cues during two-cue MWM probe trials after initially discovering the escape platform was not present, possibly indicating that the length of probe trials was too long, which may have masked any true effects. Alternately, the goal and lure cue patterns may not have been visually distinct enough, making it impossible for the mice to associate one of the visual patterns with escape consistently. Robinson, Bridge, and

Riedel (2001) tested the visual acuity of rodents by employing a cued MWM task similar to the one used in this experiment, reliably marking the quadrant containing the escape platform with a cue card containing 1 cm stripes, while a cue card containing either 1, 2, 3, 4, 5, or 10 cm stripes was placed in an adjacent quadrant that did not permit escape. Rats were unable to distinguish between quadrants and performed only at chance level when the lure quadrant was marked with anything less than a 4 cm grating on the cue card, suggesting that rodents may perceive narrow uniform stripes as a shade of grey rather than a distinct pattern when viewed from a distance (Robinson et al., 2001). Further, Robinson et al. (2001) note that a number of other parameters were necessary to facilitate learning of the task, and found that rodents performed very poorly unless the goal and lure quadrants were separated by a barrier to punish rats that made incorrect responses, and the quadrants were marked with cue cards larger than 20x24.5 cm in size. In any case, a number of modifications to the experimental procedure will be necessary before re-administering the two-cue MWM again in an attempt to assay procedural memory.

In contrast to the somewhat ambiguous results obtained in the two-cue MWM task, the open field exploration session administered prior to the OLT revealed a number of clear deficits in $Htt^{Q111/+}$ mice. The most robust phenotype observed in $Htt^{Q111/+}$ mice was a tendency toward hypoactivity during open field exploration, where HD mice were found to travel approximately 11% less overall than their $Htt^{+/+}$ counterparts during the 10 minute session. In addition, $Htt^{Q111/+}$ mice displayed increased levels of thigmotaxis and spent more time along the wall during the open field session compared to $Htt^{+/+}$ mice. These findings run somewhat counter to the findings obtained by Hölter et al. (2013) who found $Htt^{Q111/+}$ mice to be hypoactive but display decreased levels of thigmotaxis at nine months of age. While measurements of ambulation and central exploration in open field assays are often used to index anxiety related

behaviors in rodents (Ramos, 2008; Simon et al., 1994) it can be argued that any number of HD related deficits, either combined or in isolation, might contribute to the altered exploratory behaviors observed in $Htt^{Q111/+}$ mice. Psychiatric symptoms such as apathy and depression can emerge during both the pre-manifest and early stages of human HD (Epping et al., 2016; Tabrizi et al., 2009), and may contribute to the alterations in exploratory behaviors observed in $Htt^{Q111/+}$ mice during open field exploration.

To discriminate between these potential causes, comparisons were made between $Htt^{Q111/+}$ and $Htt^{+/+}$ mice regarding the total amount of time spent exploring the arena and the average velocity while exploring during the open field session. $Htt^{Q111/+}$ mice appeared to spend less time overall exploring the during the open field session, although this failed to achieve statistical significance. Further, $Htt^{Q111/+}$ mice displayed reduced velocity while exploring the open field apparatus compared to $Htt^{+/+}$ mice, which also mirrors the results obtained by Hölter et al. (2013). Although this finding suggests that a subtle motor phenotype that may contribute to the hypoactivity and reduced exploration time observed during open field testing, it is also possible that other ethological parameters, such as increased levels of stretched attend posturing, was interpreted as movement by the video tracking software and contributed to the reduced velocity observed in $Htt^{Q111/+}$ mice. Stretched attend posturing in rodents is interpreted as a risk-assessment behavior that usually occurs in tandem with an increase in other anxiety related behaviors, including a reduction in movement (Rodgers & Cole, 1993). Prior research has generally failed to observe any motor related deficits in $Htt^{Q111/+}$ mice until very late in their lifespan, further suggesting that the reduced velocity observed in $Htt^{Q111/+}$ mice is not caused by a motor related impairment (Menalled et al., 2009; Menalled, 2005). Altogether, the findings obtained during open field testing make it difficult to interpret whether the hypoactive phenotype

observed in $Htt^{Q111/+}$ mice stems from increased anxiety levels, increased apathy, or a subtle motor phenotype, and additional testing will be necessary to establish the cause of this deficit.

In contrast to the findings of Brito et al. (2014), no deficits were observed in $Htt^{Q111/+}$ mice when tested on the OLT. Both $Htt^{Q111/+}$ and $Htt^{+/+}$ mice displayed strong preferences for the relocated object relative to the familiar object, and no differences were observed between $Htt^{Q111/+}$ and $Htt^{+/+}$ mice regarding the strength of preference for the relocated object during the OLT probe session. Altogether, these results indicate that spatial LTM remains intact in $Htt^{Q111/+}$ mice at nine months of age. However, when the total number of investigations toward both objects were compared between genotypes, $Htt^{Q111/+}$ mice were found to investigate both objects roughly 16% less overall compared to their $Htt^{+/+}$ counterparts, indicating a hypoactive phenotype similar to the one observed during open field testing, possibly brought on by decreased motivation, increased anxiety levels, or a subtle motor deficit. Roy and Chapillon (2004) argue that spatial tasks relying on the tendency for rodents to explore novelty also assess emotional reactivity, and found that increased postnatal handling of rats, which reduces emotional response, increased the amount of time spent exploring a novel object in comparison to a second group of rats that had not been handled and remained largely inactive. This suggests that a lack of exploration, which can also manifest as a lack of preference for an object, should not be interpreted solely as a spatial LTM impairment (Roy & Chapillion, 2004). These findings also call into question the validity of the interpretations made by other researchers who have found spatial LTM deficits in $Htt^{Q111/+}$ mice on these types of tasks previously but did not report the number of investigations made toward each object (Brito et al., 2014; Giralt, 2008). Further testing will be necessary to ensure that the spatial LTM deficits measured on these tasks do not

stem from increased apathy or anxiety, leading to a subsequent decrease in total explorations toward the objects overall.

Given that the statistical power of an experiment can significantly alter whether the results obtained reflect a true effect (Button et al. 2013), power analyses were conducted to help aid in the interpretation of the findings obtained in this experiment as well as provide a set of best practice guidelines for using the *Htt*$^{Q111/+}$ mouse model in future behavioral research. The results of these power analyses suggested that the assays that revealed the most robust behavioral phenotypes (i.e. hypoactivity during both the open field session and OLT) achieved roughly 70% statistical power, and a group of 75 animals (~37 per genotype) would be sufficient to obtain 80% statistical power. Conversely, the two phenotypes that showed smaller effect sizes (i.e. reduced velocity and increased thigmotaxis during open field testing) achieved only 56% statistical power, suggesting that a group size of 110 mice (~55 per genotype) is necessary to obtain 80% statistical power. Overall, these results indicate that a large number of experimental animals are necessary to measure the relatively subtle behavioral phenotype associated with the *Htt*$^{Q111/+}$ mouse model of HD reliably, and further call into question the results obtained in experiments that utilized smaller sample sizes. The majority of studies that have reported behavioral deficits in *Htt*$^{Q111/+}$ mice have utilized fewer than 12 animals per genotype (Brito et al., 2014; Giralt et al., 2011; Yhnell et al., 2015), with the exception being Hölter et al. (2013) and Menalled et al. (2009) who used approximately 20-24 per genotype for their experiments. While behavioral research can undoubtedly be time consuming and difficult to conduct, these results cast doubt upon whether the results obtained in the studies that used smaller sample sizes reflect true effects or are instead spurious relations resulting from an underpowered experimental design.

The results obtained in this study also provide a clear direction for future experiments to be conducted in the $Htt^{Q111/+}$ mouse model of HD. Specifically, it will be important to parse out whether the hypoactive phenotype observed both during open field testing and during the OLT stems from increased anxiety, apathy, depression, or a subtle motor phenotype. Behavioral tests such as the elevated plus maze and light/dark apparatus are used to measure anxiety like phenotype in rodents (Ramos, 2008) and could be employed to validate the increased levels of thigmotaxis observed in $Htt^{Q111/+}$ mice during open field testing. The Porsolt swim test, a measure of behavioral despair used to measure depressive like symptoms in rodents (Castagné, Porsolt, & Moser, 2006), could similarly be used to see whether the hypoactive phenotype observed in $Htt^{Q111/+}$ mice is caused by increased depression levels. Lastly, motivation levels in $Htt^{Q111/+}$ mice may be assayed by utilizing a progressive ratio operant task, which requires rodents to progressively increase the number of lever presses necessary to receive a food reward (Trueman, Dunnett, & Brooks, 2012). Given the subtle phenotype associated with $Htt^{Q111/+}$ mice, tasks that utilize the operant chamber to probe different cognitive functions are especially appealing because they provide well defined outcome measures, greatly reduce the variability stemming from confounding variables (e.g. handling of the animals), and are a high throughput option to collect large amounts of data in a relatively short amount of time (Trueman et al., 2012).

Lastly, it is important to identify a number of limitations that may have influenced the results obtained in this study and limited the generalizability of the findings. First, female mice were used exclusively in this experiment, which did not allow any gender effects to be identified on any of the behavioral assays. Previous research has identified gender effects on behavioral tests such as social discrimination learning in males (Hölter et al., 2013), and the accelerating

rotarod at very late ages in females (Menalled et al., 2009). While no gender effects have yet been reported in $Htt^{Q111/+}$ mice during open field testing or the OLT, the possibility exists that gender effects exist on these tasks that were missed by omitting male mice from the experiment. A second potential limitation stems from the experimental animals that were used in this study. All experimental animals that were used in this experiment came from the control arm of a concurrent study assessing the efficacy of peripheral injections of antisense oligonucleotides (ASO) as a treatment for HD. This means that each experimental animal was subjected to a weekly control ASO or saline injection beginning at two months of age, making it possible that the increased handling or stress that was induced from these weekly injections differentially affected $Htt^{Q111/+}$ and $Htt^{+/+}$ mice and potentially confounded the results of the experiment. Finally, the order that the behavioral tests were administered may have affected the outcome of the behavioral tests. Since the main objective of this thesis was to identify behavioral tests sensitive to measuring cortico-striatal dysfunction, the two-cue MWM test was administered first, followed by the open field test and OLT. It is possible that exposing the experimental animals to a water based task such as the two-cue MWM may have elevated stress levels and influenced the results of the subsequent assays.

The results obtained in this experiment suggest a number of robust behavioral phenotypes in $Htt^{Q111/+}$ mice that more closely resemble features of the pre-manifest stage of the disease than traditionally used measures such as motor function and survival rate. Specifically, $Htt^{Q111/+}$ mice display increased hypoactivity, increased anxiety, and decreased velocity compared to $Htt^{+/+}$ mice, although further testing will be necessary to uncover the cause of these phenotypes. Further, a series of power analyses conducted upon the data collected in this experiment also provide improved guidelines regarding the number of experimental animals that are necessary to

achieve reliable results using the *Htt*$^{Q111/+}$ mice in future studies. Given that pre-clinical HD research stands the greatest chance of successfully translating to humans if researchers select animal models that are genetically faithful and clinical endpoints that measure the earliest and subtlest pathogenic changes, the results obtained in the current study provide an important platform for improving the quality of pre-clinical behavioral research conducted in the *Htt*$^{Q111/+}$ mouse model of HD in the future.

References

André, V. M., Cepeda, C., & Levine, M. S. (2010). Dopamine and glutamate in Huntington's disease: A balancing act. *CNS neuroscience & therapeutics*,*16*(3), 163-178.

Arrasate, M., Mitra, S., Schweitzer, E. S., Segal, M. R., & Finkbeiner, S. (2004). Inclusion body formation reduces levels of mutant huntingtin and the risk of neuronal death. *Nature*, *431*(7010), 805-810.

Azambuja, M. J., Haddad, M. S., Radanovic, M., Barbosa, E. R., & Mansur, L. L. (2007). Semantic, phonologic, and verb fluency in Huntington's disease. *Dementia Neur J*, *1*(1), 381-385.

Baldo, J. V., Schwartz, S., Wilkins, D., & Dronkers, N. F. (2006). Role of frontal versus temporal cortex in verbal fluency as revealed by voxel-based lesion symptom mapping. *Journal of the International Neuropsychological Society*, *12*(06), 896-900.

Barnes, G. T., Duyao, M. P., Ambrose, C. M., McNeil, S., Persichetti, F., Srinidhi, J., ... & MacDonald, M. E. (1994). Mouse Huntington's disease gene homolog (Hdh). *Somatic cell and molecular genetics*, *20*(2), 87-97.

Beal, M. F., & Ferrante, R. J. (2004). Experimental therapeutics in transgenic mouse models of Huntington's disease. *Nature Reviews Neuroscience*, *5*(5), 373-384.

Beste, C., Wascher, E., Dinse, H. R., & Saft, C. (2012). Faster perceptual learning through excitotoxic neurodegeneration. *Current Biology*, *22*(20), 1914-1917.

Bonner-Jackson, A., Long, J. D., Westervelt, H., Tremont, G., Aylward, E., & Paulsen, J. S. (2013). Cognitive reserve and brain reserve in prodromal Huntington's disease. *Journal of the International Neuropsychological Society*, *19*(07), 739-750.

Brito, V., Giralt, A., Enriquez-Barreto, L., Puigdellívol, M., Suelves, N., Zamora-Moratalla, A., ... & Alberch, J. (2014). Neurotrophin receptor p75 (NTR) mediates Huntington's disease-associated synaptic and memory dysfunction. *The Journal of clinical investigation*, *124*(10), 4411-4428.

Button, K. S., Ioannidis, J. P., Mokrysz, C., Nosek, B. A., Flint, J., Robinson, E. S., & Munafò, M. R. (2013). Power failure: why small sample size undermines the reliability of neuroscience. *Nature Reviews Neuroscience*, *14*(5), 365-376.

Castagné, V., Porsolt, R. D., & Moser, P. (2006). Early behavioral screening for antidepressants and anxiolytics. *Drug development research*, *67*(9), 729-742.

Chapleau, C. A., & Pozzo-Miller, L. (2012). Divergent roles of p75 NTR and Trk receptors in BDNF's effects on dendritic spine density and morphology. *Neural plasticity*, *2012*.

Chen, J. Y., Wang, E. A., Cepeda, C., & Levine, M. S. (2013). Dopamine imbalance in Huntington's disease: a mechanism for the lack of behavioral flexibility. *Frontiers in neuroscience*, *7*, 114, 1-8.

Cohen, M. X., & Frank, M. J. (2009). Neurocomputational models of basal ganglia function in learning, memory and choice. *Behavioural brain research*,*199*(1), 141-156.

Cools, R., Barker, R. A., Sahakian, B. J., & Robbins, T. W. (2001). Enhanced or impaired cognitive function in Parkinson's disease as a function of dopaminergic medication and task demands. *Cerebral Cortex*, *11*(12), 1136-1143.

Deng, Y. P., Albin, R. L., Penney, J. B., Young, A. B., Anderson, K. D., & Reiner, A. (2004). Differential loss of striatal projection systems in Huntington's disease: a quantitative immunohistochemical study. *Journal of chemical neuroanatomy*, *27*(3), 143-164.

Dunlap, C. B. (1927). Pathologic changes in Huntington's chorea: with special reference to the corpus striatum. *Archives of Neurology & Psychiatry*, *18*(6), 867-943.

Duyao, M. P., Auerbach, A. B., Ryan, A., Persichetti, F., Barnes, G. T., McNeil, S. M., ... & Joyner, A. L. (1995). Inactivation of the mouse Huntington's disease gene homolog Hdh. *Science*, *269*(5222), 407-410.

Ehrnhoefer, D. E., Butland, S. L., Pouladi, M. A., & Hayden, M. R. (2009). Mouse models of Huntington disease: variations on a theme. *Disease Models and Mechanisms*, *2*(3-4), 123-129.

Epping, E. A., Kim, J. I., Craufurd, D., Brashers-Krug, T. M., Anderson, K. E., McCusker, E., ... & Coordinators of the Huntington Study Group. (2016). Longitudinal Psychiatric Symptoms in Prodromal Huntington's Disease: A Decade of Data. *American Journal of Psychiatry*.

Estrada-Sánchez, A. M., Burroughs, C. L., Cavaliere, S., Barton, S. J., Chen, S., Yang, X. W., & Rebec, G. V. (2015). Cortical Efferents Lacking Mutant huntingtin Improve Striatal Neuronal Activity and Behavior in a Conditional Mouse Model of Huntington's Disease. *The Journal of Neuroscience*, *35*(10), 4440-4451.

Frank, M. J. (2006). Hold your horses: a dynamic computational role for the subthalamic nucleus in decision making. *Neural Networks*, *19*(8), 1120-1136.

Gines, S., Seong, I. S., Fossale, E., Ivanova, E., Trettel, F., Gusella, J. F., ... & MacDonald, M. E. (2003). Specific progressive cAMP reduction implicates energy deficit in presymptomatic Huntington's disease knock-in mice. *Human molecular genetics*, *12*(5), 497-508.

Giralt, A., Puigdellivol, M., Carretón, O., Paoletti, P., Valero, J., Parra, A., ... & Ginés, S. (2011). Long-term memory deficits in Huntington's disease are associated with reduced CBP histone acetylase activity. *Human molecular genetics*, ddr552.

Giralt, A., Saavedra, A., Alberch, J., & Pérez-Navarro, E. (2012). Cognitive dysfunction in Huntington's disease: humans, mouse models and molecular mechanisms. *Journal of Huntington's disease*, *1*(2), 155-173.

Gold, P. E. (2004). Coordination of multiple memory systems. *Neurobiology of learning and memory*, *82*(3), 230-242.

Harjes, P., & Wanker, E. E. (2003). The hunt for huntingtin function: interaction partners tell many different stories. *Trends in biochemical sciences*, *28*(8), 425-433.

Hartley, T., & Burgess, N. (2005). Complementary memory systems: competition, cooperation and compensation. *Trends in Neurosciences*, *28*(4), 169-170.

Ho, A. K., Sahakian, B. J., Robbins, T. W., Barker, R. A., Rosser, A. E., & Hodges, J. R. (2002). Verbal fluency in Huntington's disease: a longitudinal analysis of phonemic and semantic clustering and switching. *Neuropsychologia*, *40*(8), 1277-1284.

Hockly, E., Cordery, P. M., Woodman, B., Mahal, A., Van Dellen, A., Blakemore, C., ... & Bates, G. P. (2002). Environmental enrichment slows disease progression in R6/2 Huntington's disease mice. *Annals of neurology*,*51*(2), 235-242.

Hölter, S. M., Stromberg, M., Kovalenko, M., Garrett, L., Glasl, L., Lopez, E., ... & Rozman, J. (2013). A broad phenotypic screen identifies novel phenotypes driven by a single mutant allele in Huntington's disease CAG knock-in mice. *PloS one*, *8*(11), e80923.

Huntington, G. (1872). On chorea. *The medical and surgical reporter: a weekly journal*, 26(15), 317-321.

Ioannidis, J. P. (2005). Why most published research findings are false.*PLoS Med*, *2*(8), e124.

Labuschagne, I., Jones, R., Callaghan, J., Whitehead, D., Dumas, E. M., Say, M. J., ... & Frost, C. (2013). Emotional face recognition deficits and medication effects in pre-manifest through stage-II Huntington's disease. *Psychiatry research*, *207*(1), 118-126.

Lawrence, A. D., Sahakian, B. J., & Robbins, T. W. (1998). Cognitive functions and corticostriatal circuits: insights from Huntington's disease. *Trends in cognitive sciences*, *2*(10), 379-388.

Lawrence, A. D., Weeks, R. A., Brooks, D. J., Andrews, T. C., Watkins, L. H., Harding, A. E., ... & Sahakian, B. J. (1998). The relationship between striatal dopamine receptor binding and cognitive performance in Huntington's disease. *Brain*, *121*(7), 1343-1355.

Lee, A. S., Duman, R. S., & Pittenger, C. (2008). A double dissociation revealing bidirectional competition between striatum and hippocampus during learning. *Proceedings of the National Academy of Sciences*, *105*(44), 17163-17168.

Li, S. H., & Li, X. J. (2004). Huntington and its role in neuronal degeneration. *The Neuroscientist*, *10*(5), 467-475.

Liot, G., Zala, D., Pla, P., Mottet, G., Piel, M., & Saudou, F. (2013). Mutant Huntingtin alters retrograde transport of TrkB receptors in striatal dendrites. *The Journal of Neuroscience*, *33*(15), 6298-6309.

Loy, C. T., & McCusker, E. A. (2013). Is a motor criterion essential for the diagnosis of clinical huntington disease? *PLoS currents*, *5*.

Lu, B., Nagappan, G., Guan, X., Nathan, P. J., & Wren, P. (2013). BDNF-based synaptic repair as a disease-modifying strategy for neurodegenerative diseases. *Nature Reviews Neuroscience*, *14*(6), 401-416.

MacDonald, M. E., Ambrose, C. M., Duyao, M. P., Myers, R. H., Lin, C., Srinidhi, L., ... & Groot, N. The Huntington's Disease Collaborative Research Group (1993) A novel gene containing a trinucleotide repeat that is expanded and unstable on Huntington's disease chromosomes. *Cell*, *72*(6), 971-983.

Malenka, R. C., & Nicoll, R. A. (1999). Long-term potentiation- a decade of progress? *Science*, *285*(5435), 1870-1874.

Menalled, L. B. (2005). Knock-in mouse models of Huntington's disease. *NeuroRx*, *2*(3), 465-470.

Menalled, L., & Brunner, D. (2014). Animal models of Huntington's disease for translation to the clinic: best practices. *Movement Disorders*, *29*(11), 1375-1390.

Menalled, L. B., & Chesselet, M. F. (2002). Mouse models of Huntington's disease. *Trends in pharmacological sciences*, *23*(1), 32-39.

Menalled, L., El-Khodor, B. F., Patry, M., Suárez-Fariñas, M., Orenstein, S. J., Zahasky, B., ... & Morton, A. J. (2009). Systematic behavioral evaluation of Huntington's disease transgenic and knock-in mouse models.*Neurobiology of disease*, *35*(3), 319-336.

Menalled, L., Lutz, C., Ramboz, S., Brunner, D., Lager, B., Noble, S., ... & Howland, D. (2014). A Field Guide to Working with Mouse Models of Huntington's Disease.

Milnerwood, A. J., Cummings, D. M., Dallérac, G. M., Brown, J. Y., Vatsavayai, S. C., Hirst, M. C., ... & Murphy, K. P. (2006). Early development of aberrant synaptic plasticity in a mouse model of Huntington's disease. *Human molecular genetics*, *15*(10), 1690-1703.

Milnerwood, A. J., & Raymond, L. A. (2010). Early synaptic pathophysiology in neurodegeneration: Insights from Huntington's disease. *Trends in neurosciences*, *33*(11), 513-523.

Mink, J. W. (1996). The basal ganglia: focused selection and inhibition of competing motor programs. *Progress in neurobiology*, *50*(4), 381-425.

Montoya, A., Pelletier, M., Menear, M., Duplessis, E., Richer, F., & Lepage, M. (2006). Episodic memory impairment in Huntington's disease: a meta-analysis. *Neuropsychologia*, *44*(10), 1984-1994.

Murai, T., Okuda, S., Tanaka, T., & Ohta, H. (2006). Behavioral characterization of the object location test in mice. *Journal of Pharmocological Sciences, 100,* 116-124.

Noldus, L. P., Spink, A. J., & Tegelenbosch, R. A. (2001). EthoVision: a versatile video tracking system for automation of behavioral experiments.*Behavior Research Methods, Instruments, & Computers*, *33*(3), 398-414.

Novak, M. J., Warren, J. D., Henley, S. M., Draganski, B., Frackowiak, R. S., & Tabrizi, S. J. (2012). Altered brain mechanisms of emotion processing in pre-manifest Huntington's disease. *Brain*, *135*(4), 1165-1179.

Orth, M., Schippling, S., Schneider, S. A., Bhatia, K. P., Talelli, P., Tabrizi, S. J., & Rothwell, J. C. (2010). Abnormal motor cortex plasticity in premanifest and very early manifest Huntington disease. *Journal of Neurology, Neurosurgery & Psychiatry*, *81*(3), 267-270.

Papoutsi, M., Labuschagne, I., Tabrizi, S. J., & Stout, J. C. (2014). The cognitive burden in Huntington's disease: pathology, phenotype, and mechanisms of compensation. *Movement Disorders*, *29*(5), 673-683.

Paulsen, J. S. (2011). Cognitive impairment in Huntington disease: diagnosis and treatment. *Current neurology and neuroscience reports*, *11*(5), 474-483.

Penney, J. B., Vonsattel, J. P., Macdonald, M. E., Gusella, J. F., & Myers, R. H. (1997). CAG repeat number governs the development rate of pathology in Huntington's disease. *Annals of neurology*, *41*(5), 689-692.

Pittenger, C., Fasano, S., Mazzocchi-Jones, D., Dunnett, S. B., Kandel, E. R., & Brambilla, R. (2006). Impaired bidirectional synaptic plasticity and procedural memory formation in striatum-specific cAMP response element-binding protein-deficient mice. *The Journal of neuroscience*, *26*(10), 2808-2813.

Plotkin, J. L., Day, M., Peterson, J. D., Xie, Z., Kress, G. J., Rafalovich, I., ... & Stavarache, M. (2014). Impaired TrkB receptor signaling underlies corticostriatal dysfunction in Huntington's disease. *Neuron*, *83*(1), 178-188.

Plotkin, J. L., & Surmeier, D. J. (2014). Impaired striatal function in Huntington's disease is due to aberrant p75NTR signaling. *Rare Diseases*,*2*(1), e968482.

Poldrack, R. A., Clark, J., Pare-Blagoev, E. J., Shohamy, D., Moyano, J. C., Myers, C., & Gluck, M. A. (2001). Interactive memory systems in the human brain. *Nature*, *414*(6863), 546-550.

R Core Team (2015). R: A Language and Environment for Statistical Computing. Vienna, Austria: R Foundation for Statistical Computing; 2014. R Foundation for Statistical Computing.

Ramos, A. (2008). Animal models of anxiety: do I need multiple tests? *Trends in pharmacological sciences*, *29*(10), 493-498.

Redgrave, P., Gurney, K., & Reynolds, J. (2008). What is reinforced by phasic dopamine signals? *Brain research reviews*, *58*(2), 322-339.

Redgrave, P., Rodriguez, M., Smith, Y., Rodriguez-Oroz, M. C., Lehericy, S., Bergman, H., ... & Obeso, J. A. (2010). Goal-directed and habitual control in the basal ganglia: implications for Parkinson's disease. *Nature Reviews Neuroscience*, *11*(11), 760-772.

Reilmann, R., Leavitt, B. R., & Ross, C. A. (2014). Diagnostic criteria for Huntington's disease based on natural history. *Movement Disorders*, *29*(11), 1335-1341.

Robinson, L., Bridge, H., & Riedel, G. (2001). Visual discrimination learning in the water maze: a novel test for visual acuity. *Behavioural brain research*,*119*(1), 77-84.

Rodgers, R. J., & Cole, J. C. (1993). Anxiety enhancement in the murine elevated plus maze by immediate prior exposure to social stressors. *Physiology & behavior*, *53*(2), 383-388.

Rosas, H. D., Koroshetz, W. J., Chen, Y. I., Skeuse, C., Vangel, M., Cudkowicz, M. E., ... & Jenkins, B. G. (2003). Evidence for more widespread cerebral pathology in early HD: An MRI-based morphometric analysis. *Neurology*, *60*(10), 1615-1620.

Rosas, H. D., Salat, D. H., Lee, S. Y., Zaleta, A. K., Pappu, V., Fischl, B., ... & Hersch, S. M. (2008). Cerebral cortex and the clinical expression of Huntington's disease: complexity and heterogeneity. *Brain*, *131*(4), 1057-1068.

Roy, V., & Chapillon, P. (2004). Further evidences that risk assessment and object exploration behaviours are useful to evaluate emotional reactivity in rodents. *Behavioural brain research*, *154*(2), 439-448.

Simon, P., Dupuis, R., & Costentin, J. (1994). Thigmotaxis as an index of anxiety in mice. Influence of dopaminergic transmissions. *Behavioural brain research*, *61*(1), 59-64.

Smith, R., Brundin, P., & Li, J. Y. (2005). Synaptic dysfunction in Huntington's disease: a new perspective. *Cellular and Molecular Life Sciences CMLS*, *62*(17), 1901-1912.

Tabrizi, S. J., Langbehn, D. R., Leavitt, B. R., Roos, R. A., Durr, A., Craufurd, D., ... & Borowsky, B. (2009). Biological and clinical manifestations of Huntington's disease in the longitudinal TRACK-HD study: cross-sectional analysis of baseline data. *The Lancet Neurology*, *8*(9), 791-801.

Tabrizi, S. J., Scahill, R. I., Owen, G., Durr, A., Leavitt, B. R., Roos, R. A., ... & Craufurd, D. (2013). Predictors of phenotypic progression and disease onset in premanifest and early-stage Huntington's disease in the TRACK-HD study: analysis of 36-month observational data. *The Lancet Neurology*,*12*(7), 637-649.

Tang, C. C., Feigin, A., Ma, Y., Habeck, C., Paulsen, J. S., Leenders, K. L., ... & Eidelberg, D. (2013). Metabolic network as a progression biomarker of premanifest Huntington's disease. *The Journal of clinical investigation*, *123*(9), 4076-4088.

Trueman, R. C., Dunnett, S. B., & Brooks, S. P. (2012). Operant-based instrumental learning for analysis of genetically modified models of Huntington's disease. *Brain research bulletin*, *88*(2), 261-275.

Voermans, N. C., Petersson, K. M., Daudey, L., Weber, B., Van Spaendonck, K. P., Kremer, H. P., & Fernández, G. (2004). Interaction between the human hippocampus and the caudate nucleus during route recognition. *Neuron*, *43*(3), 427-435.

Vonsattel, J. P., Myers, R. H., Stevens, T. J., Ferrante, R. J., Bird, E. D., & Richardson Jr, E. P. (1985). Neuropathological classification of Huntington's disease. *Journal of Neuropathology & Experimental Neurology*, *44*(6), 559-577.

Walker, F. O. (2007). Huntington's disease. *The Lancet*, *369*(9557), 218-228.

Wheeler, V. C., Auerbach, W., White, J. K., Srinidhi, J., Auerbach, A., Ryan, A., ... & Joyner, A. L. (1999). Length-dependent gametic CAG repeat instability in the Huntington's disease knock-in mouse. *Human molecular genetics*, *8*(1), 115-122.

Yhnell, E., Dunnett, S. B., & Brooks, S. P. (2015). The utilisation of operant delayed matching and non-matching to position for probing cognitive flexibility and working memory in mouse models of Huntington's disease.*Journal of neuroscience methods*.

Yin, H. H., Mulcare, S. P., Hilário, M. R., Clouse, E., Holloway, T., Davis, M. I., ... & Costa, R. M. (2009). Dynamic reorganization of striatal circuits during the acquisition and consolidation of a skill. *Nature neuroscience*, *12*(3), 333-341.

Zala, D., Colin, E., Rangone, H., Liot, G., Humbert, S., & Saudou, F. (2008). Phosphorylation of mutant huntingtin at S421 restores anterograde and retrograde transport in neurons. *Human molecular genetics*, *17*(24), 3837-3846.

Zuccato, C., Ciammola, A., Rigamonti, D., Leavitt, B. R., Goffredo, D., Conti, L., ... & Timmusk, T. (2001). Loss of huntingtin-mediated BDNF gene transcription in Huntington's disease. *Science*, *293*(5529), 493-498.

Table 1

Mean Latencies to Locate the Escape Platform during Two-cue MWM Training by Day.

	$Htt^{+/+}$	$Htt^{Q111/+}$	Total
Day	*M* (*SD*)	*M* (*SD*)	*M* (*SD*)
1	24.47 (27.41)	24.57 (28.56)	24.53 (27.97)
2	10.10 (8.65)	10.93 (8.51)	10.53 (8.57)*
3	7.15 (5.77)	8.86 (6.90)	8.05 (6.43)*
4	7.20 (5.20)	7.74 (6.47)	7.49 (5.89)*†
5	6.36 (4.61)	6.99 (7.01)	6.69 (5.98)* †
6	6.14 (4.98)	5.77 (3.91)	5.95 (4.45)* †
7	5.99 (3.89)	5.96 (4.32)	5.97 (4.11)* †

Note: Dependent variable = Latency to reach escape platform. An asterisk (*) indicates values were statistically significant from day 1 at the $p < .05$ level. A dagger (†) indicates values were statistically significant from day 2 at the $p < .05$ level.

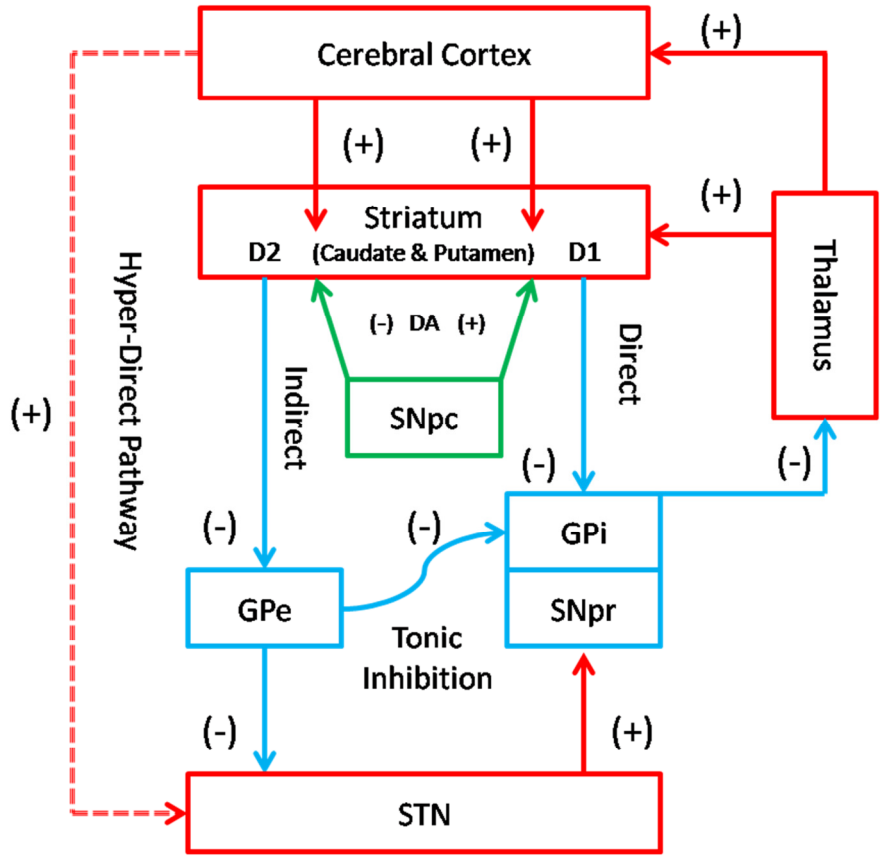

Figure 1. Schematic of the direct, indirect, hyper-direct, and dopaminergic projections within the basal ganglia. Glutamatergic connections are represented in red, GABAergic connections in blue, and dopaminergic connections in green. Activation of the "direct" pathway results in the inhibition of the GPi and SNr, followed by the disinhibition of thalamic feedback to the cerebral cortex. Activation of the "indirect" pathway removes the tonic inhibition of the GPe from the GPi and STN, further strengthening inhibition by the GPi and SNr upon the thalamus, which suppresses thalamic feedback to the cerebral cortex overall. *DA* = dopamine; *SNpc* = substantia nigra pars compacta; *SNpr* = substantia nigra pars reticulata; *GPe* = globus pallidus – external segment; *GPi* = globus pallidus – internal segment; *STN* = subthalamic nucleus. Adapted from Papoutsi et. al, (2014).

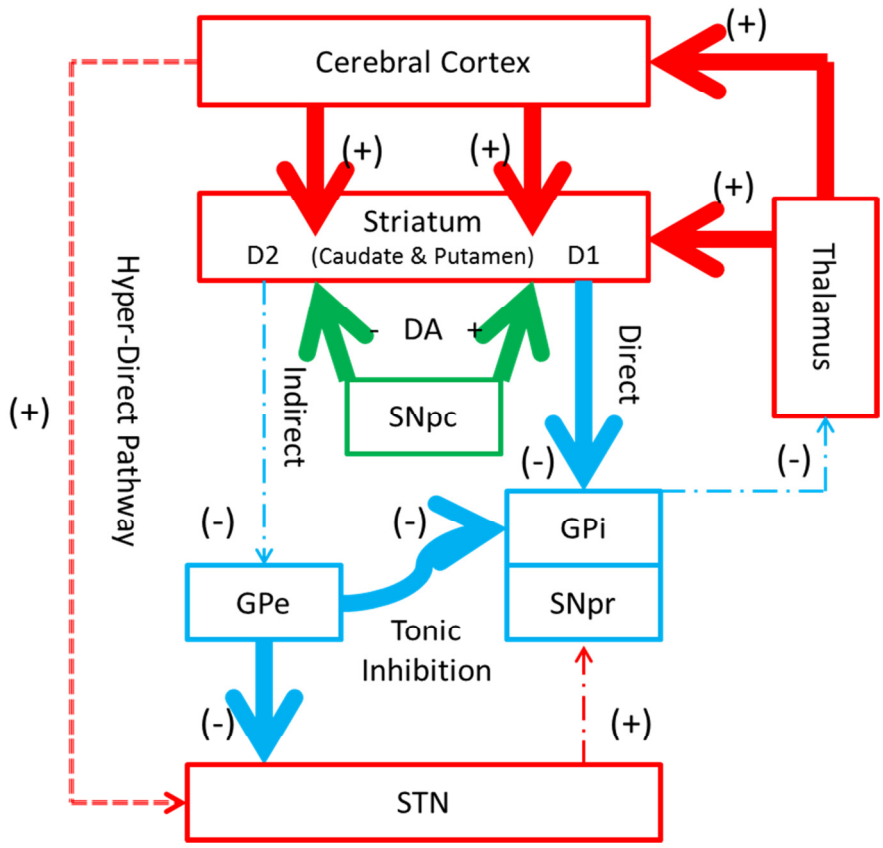

Figure 2. Schematic of the gradient of pathology observed during early manifest HD. Glutamatergic connections are represented in red, GABAergic connections in blue, and dopaminergic connections in green. Changes in signaling due to neuropathological changes are represented with either dashed lines (decrease) or bolded lines (increase.) Neurodegeneration along the indirect pathway increases the tonic inhibition of the GPe upon the GPi and STN, disinhibiting thalamic feedback to the neocortex. Concurrently, direct pathway MSNs become over activated due to increased levels of extracellular glutamate, disinhibiting the thalamus even further. *DA* = dopamine; *SNpc* = substantia nigra pars compacta; *SNpr* = substantia nigra pars reticulata; *GPe* = globus pallidus – external segment; *GPi* = globus pallidus – internal segment; *STN* = subthalamic nucleus. Adapted from Papoutsi et. al, (2014).

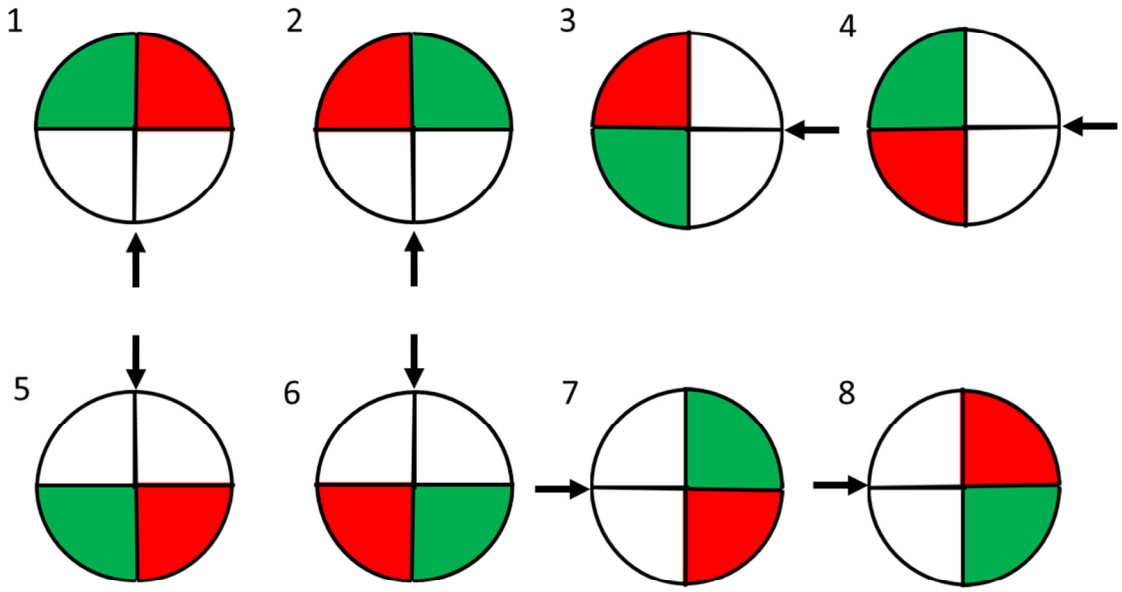

Figure 3. Schematic of the eight possible MWM orientations and entry locations. Goal cue location is shaded in green, and lure cue location is shaded in red. Entry location for each orientation is represented with an arrow. Adapted from Lee, Duman, and Pittinger (2008).

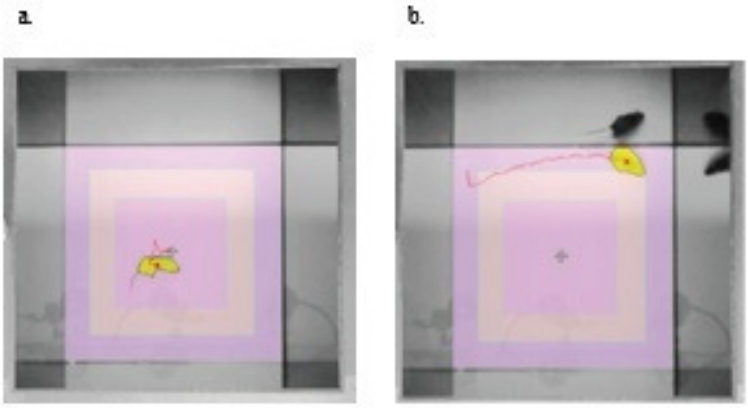

Figure 4. Visual representation of the concentric zones used to measure thigmotaxis in experimental animals. Mice were considered less anxious if they spent more time occupying the inner zone (a) than the outer zone (b).

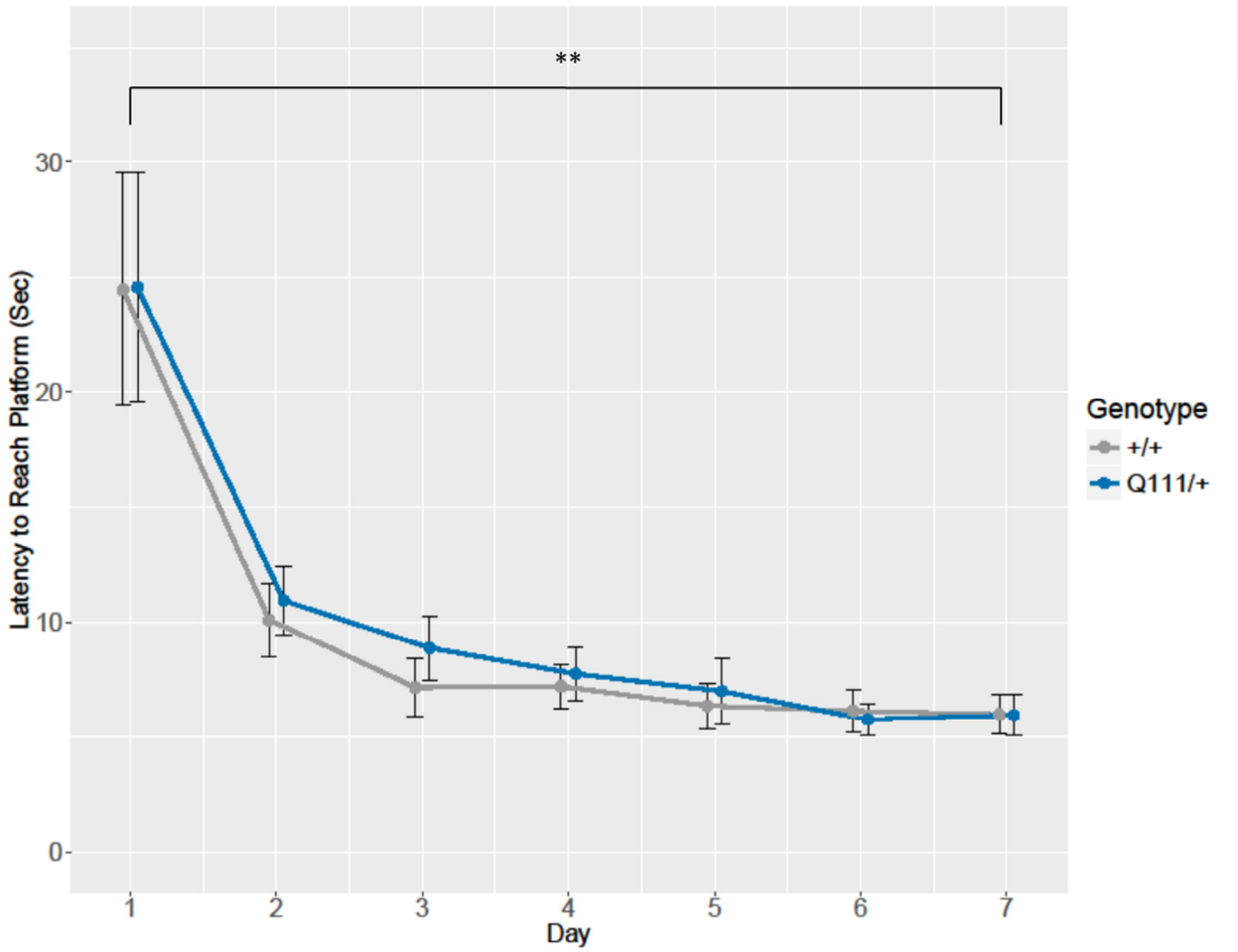

Figure 5. Average latency to reach the escape platform during two-cue Morris water maze training trials by day. Error bars represent 95% CI. A double asterisk (**) indicates values were statistically significantly different at the $p < .01$ level.

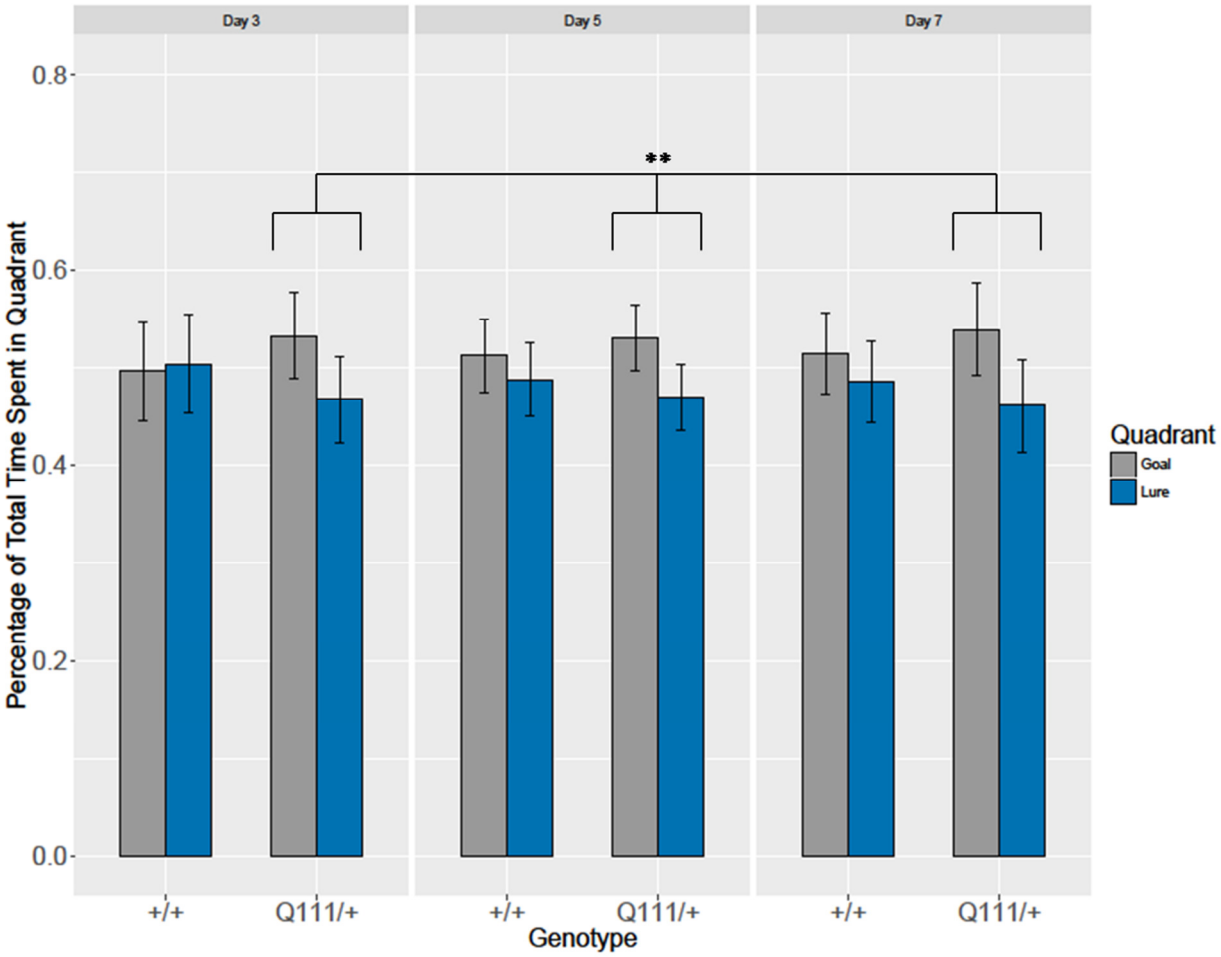

Figure 6. Percentage of total time spent in the goal and lure quadrants during two-cue MWM probe trials. Error bars represent 95% CI. A double asterisk (**) indicates post-hoc simple effects were statistically significant at the $p < .01$ level.

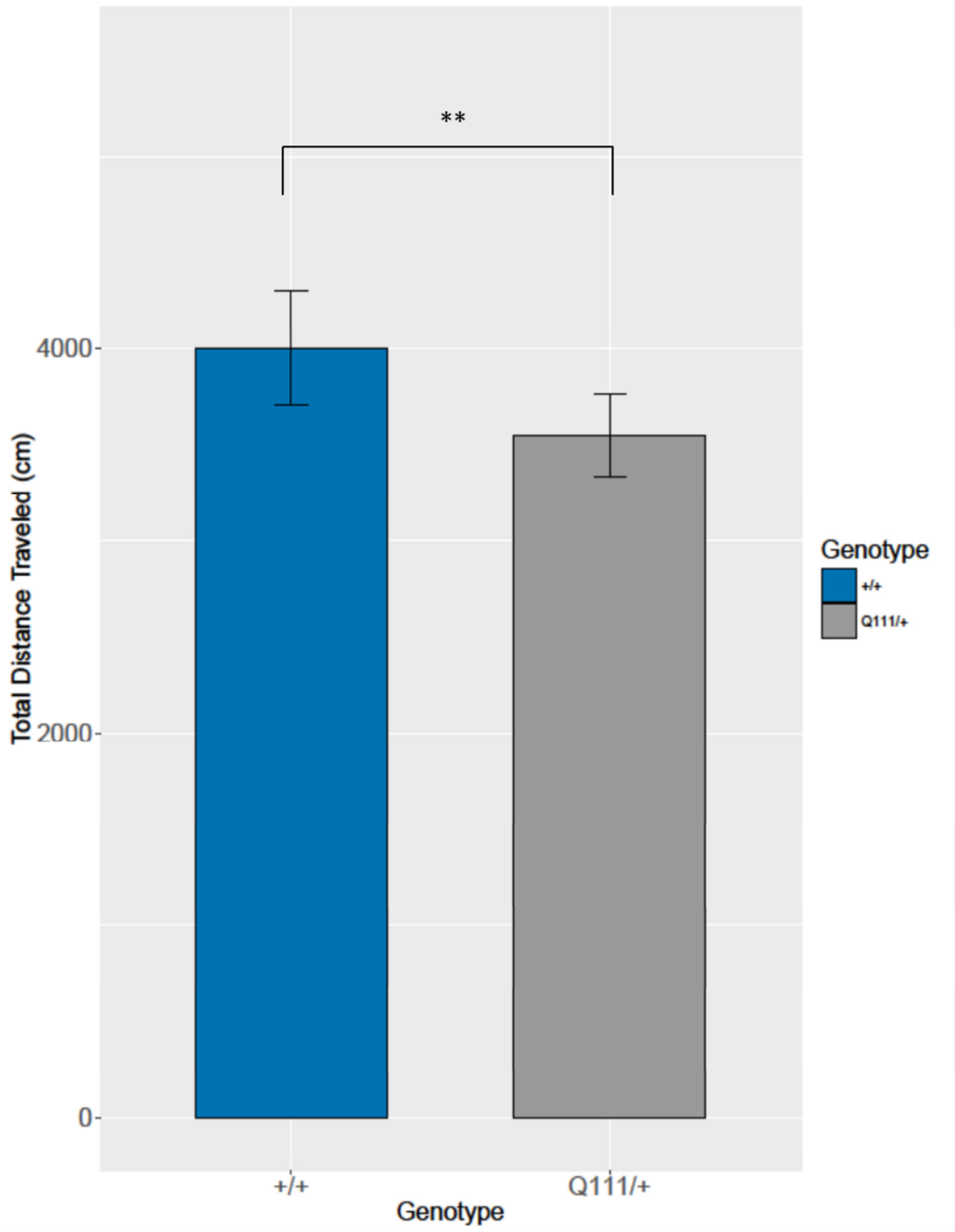

Figure 7. Total distance traveled (cm) by $Htt^{+/+}$ and $Htt^{Q111/+}$ mice during the OF session. Error bars represent 95% CI. A double asterisk (**) indicates values were statistically significant at the $p = .01$ level.

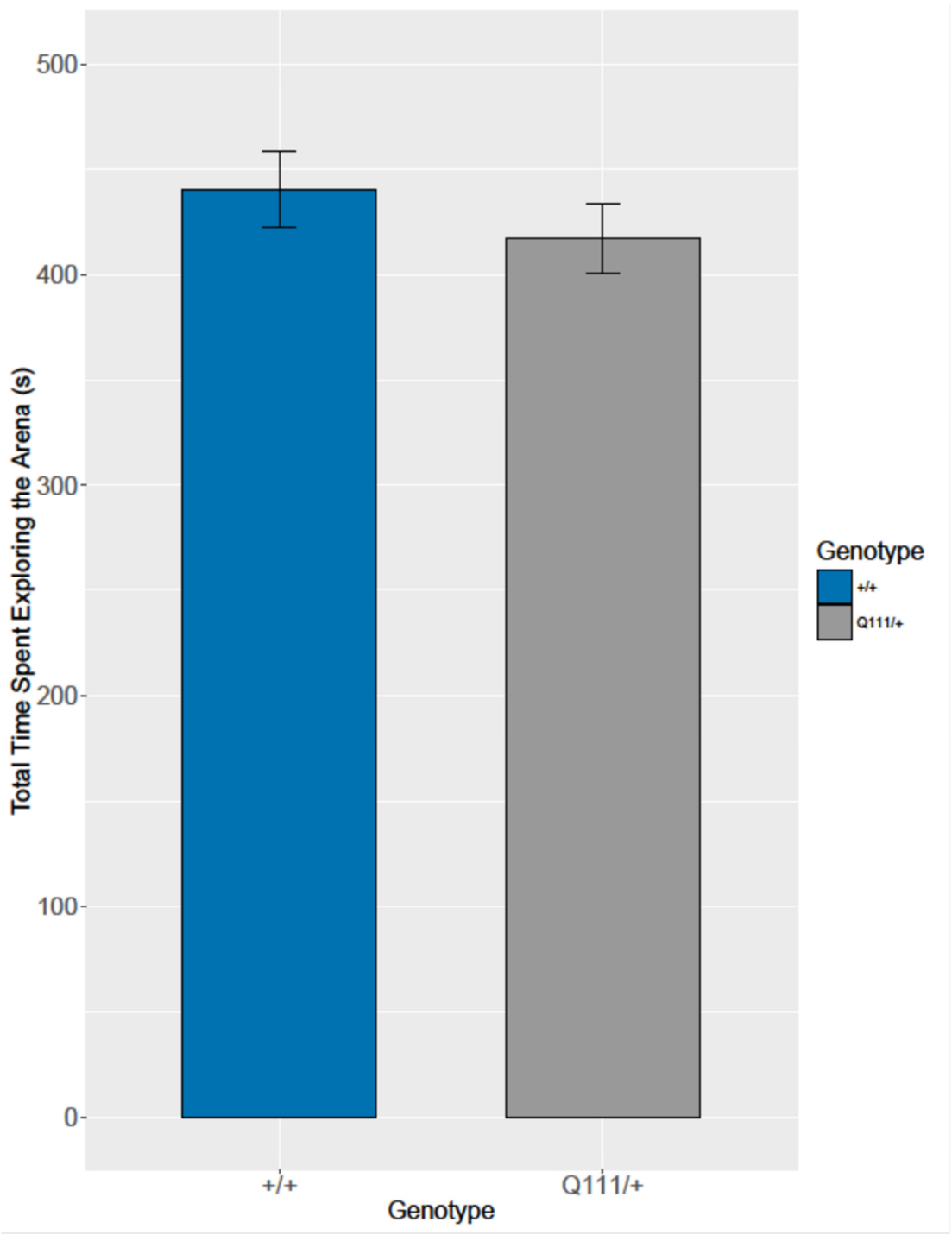

Figure 8. Total time spent actively exploring by $Htt^{+/+}$ and $Htt^{Q111/+}$ mice during the open field session. Error bars represent 95% CI.

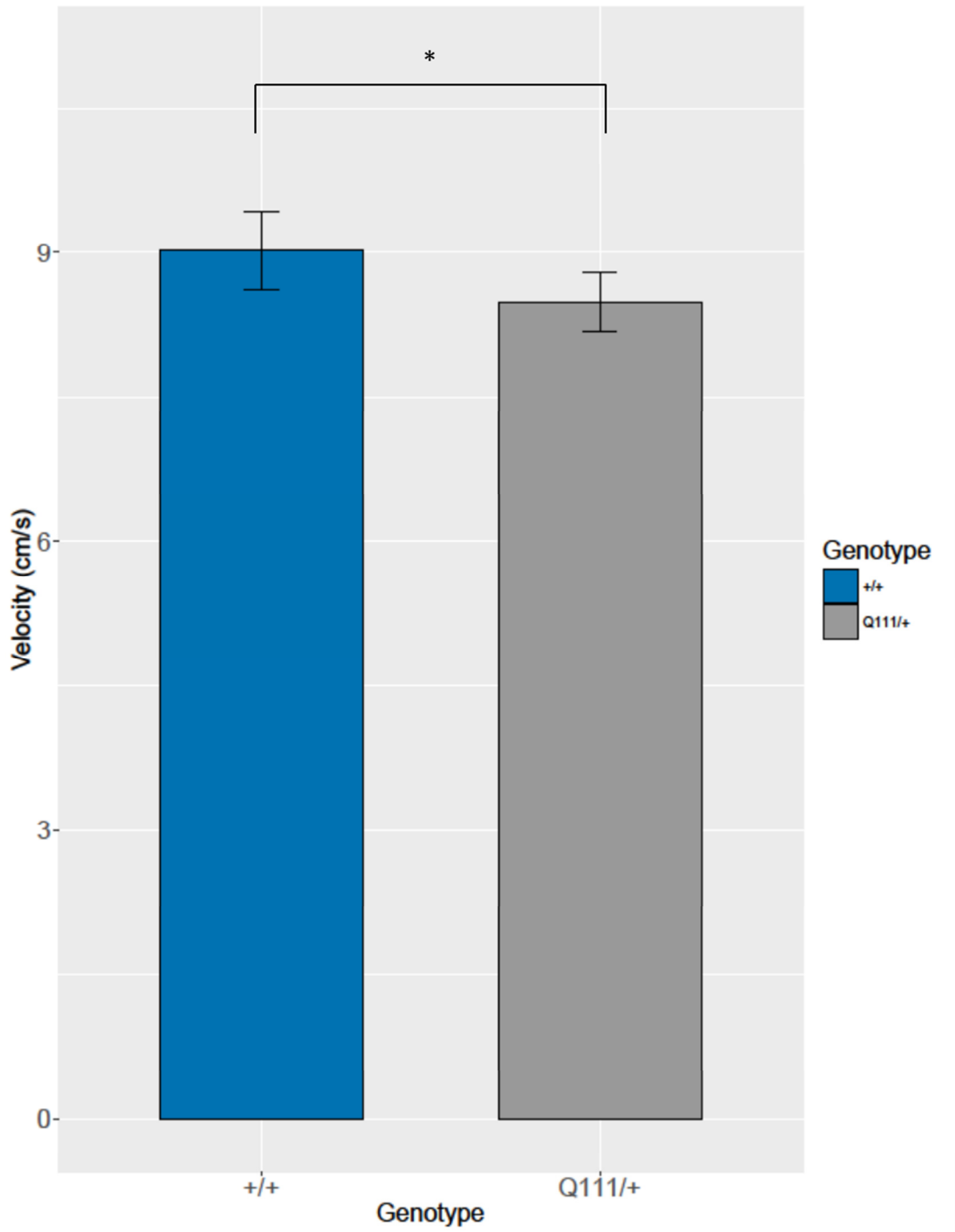

Figure 9. Average velocity (cm/s) of $Htt^{+/+}$ and $Htt^{Q111/+}$ mice during the open field session. Error bars represent 95% CI. An asterisk (*) indicates values were statistically significant at the $p < .05$ level.

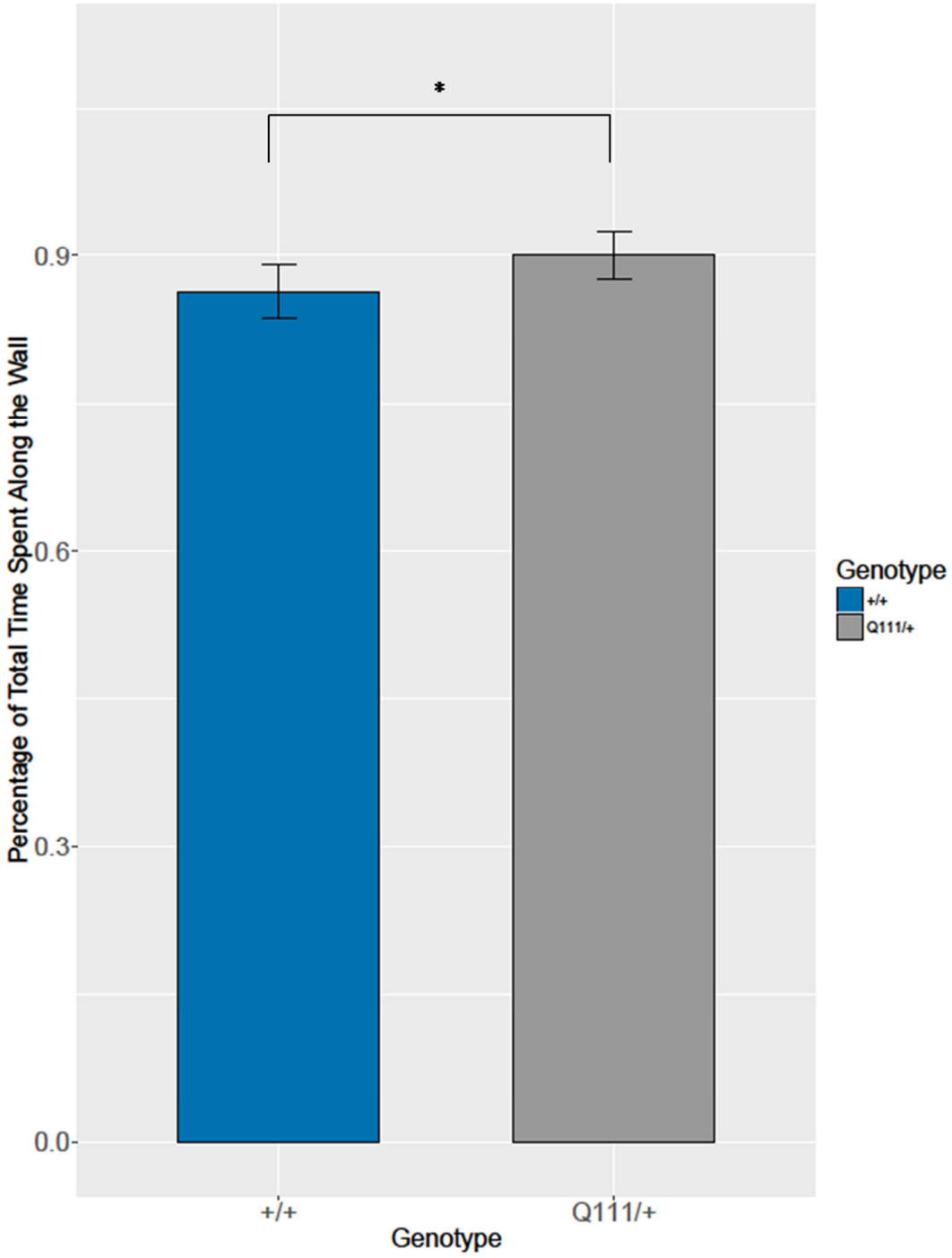

Figure 10. Percentage of total time spent along the wall by $Htt^{+/+}$ and $Htt^{Q111/+}$ mice during the open field session. Error bars represent 95% CI. An asterisk (*) indicates values were statistically significant at the $p < .05$ level.

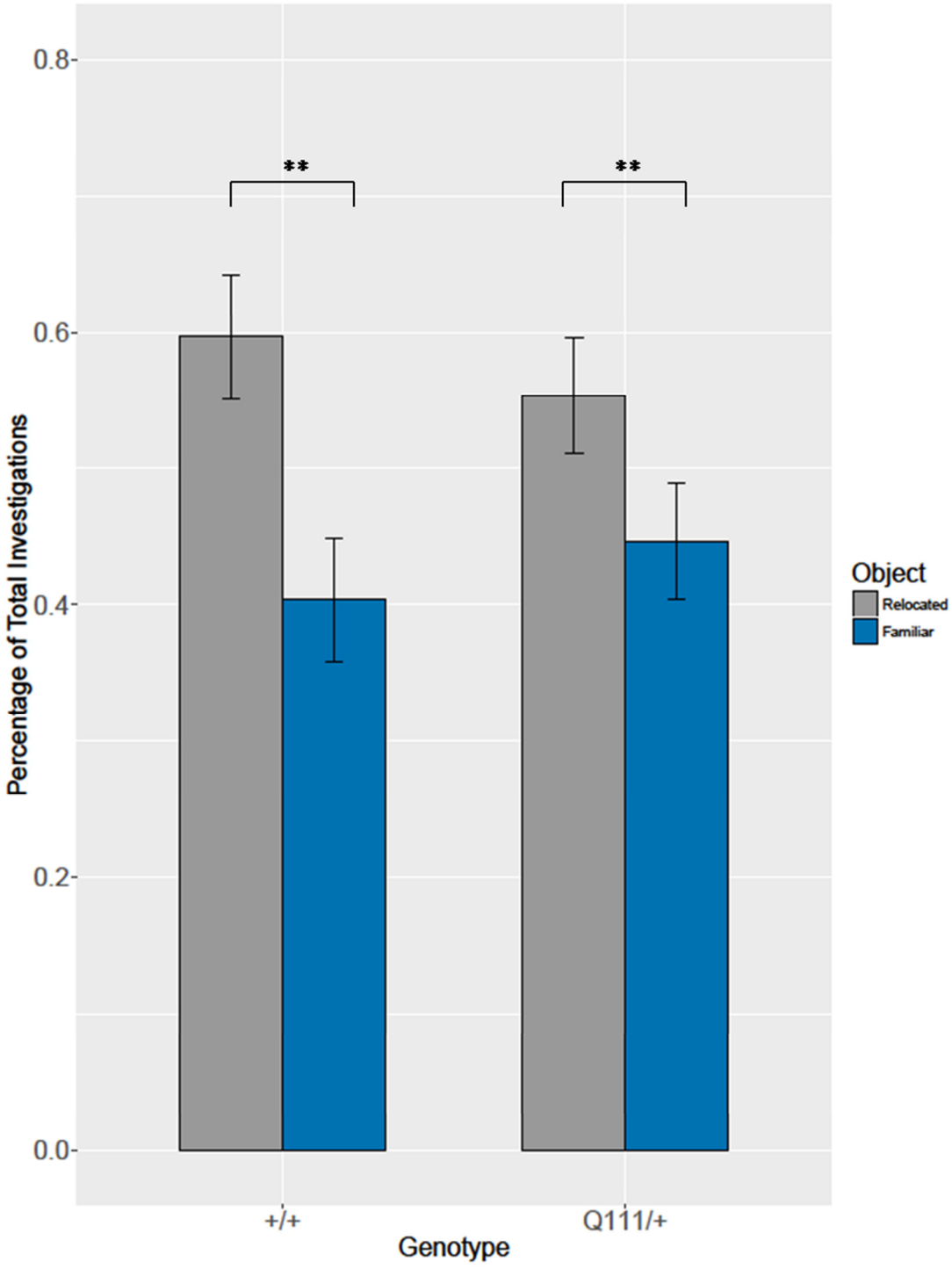

Figure 11. Percentage of total investigations by $Htt^{+/+}$ and $Htt^{Q111/+}$ mice to the familiar and relocated objects during the OLT. Error bars represent 95% CI. A double asterisk (**) indicates values were statistically significant at the $p = .01$ level.

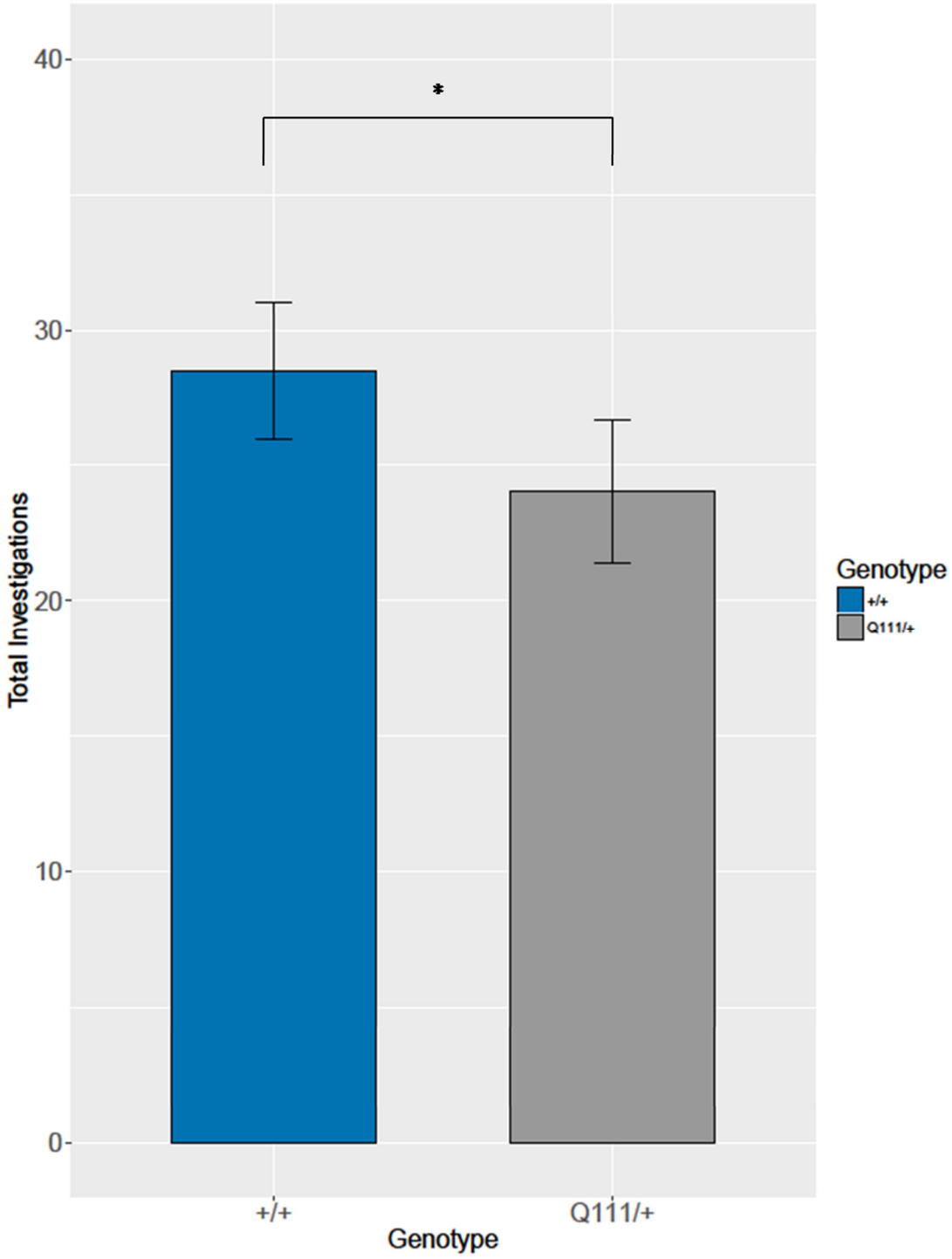

Figure 12. Total number of investigations to the familiar and relocated objects by $Htt^{+/+}$ and $Htt^{Q111/+}$ mice during the OLT. Error bars represent 95% CI. An asterisk (*) indicates values were statistically significant at the $p < .05$ level.